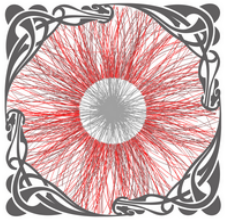

XXIV QUARK MATTER
DARMSTADT 2014

# *Measurement of the long-range pseudorapidity correlations and azimuthal harmonics in $\sqrt{s}$=5.02 TeV proton-lead collisions with the ATLAS detector*

Sooraj Radhakrishnan

for the ATLAS Collaboration

ATLAS-COM-CONF-2014-026

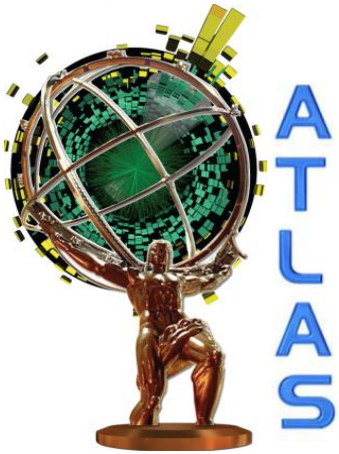


Stony Brook
University

# Introduction: Ridge in p + Pb collisions

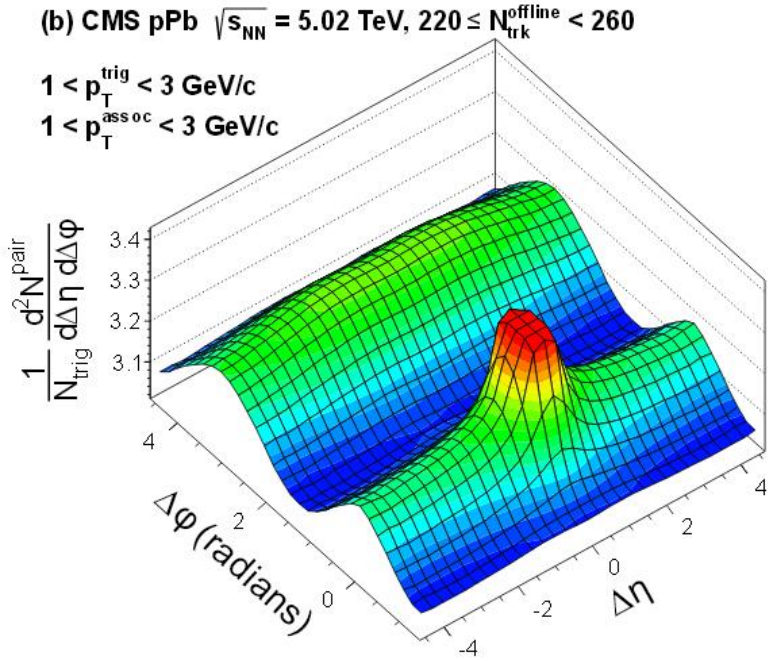


- Intriguing long range correlation ("ridge") seen in two particle angular correlations in high multiplicity p+Pb collisions.
- Peripheral subtraction revealed "double ridge".
- Arising from correlations in the initial state or through final state interactions??

- Dedicated p+Pb run at LHC in 2013

  $\sqrt{s_{NN}} = 5.02$ TeV, Integrated Luminosity ~28 $nb^{-1}$

- What is new:
  - Measurements extended to higher $p_T$ than existing results employing a recoil subtraction procedure.
  - First 5 Fourier harmonics associated with the long-range correlations, for two different 'event-activity' definitions.
  - Comparison of $v_n$ values between p+Pb and peripheral Pb+Pb collisions with comparable multiplicity

# ATLAS detector and dataset

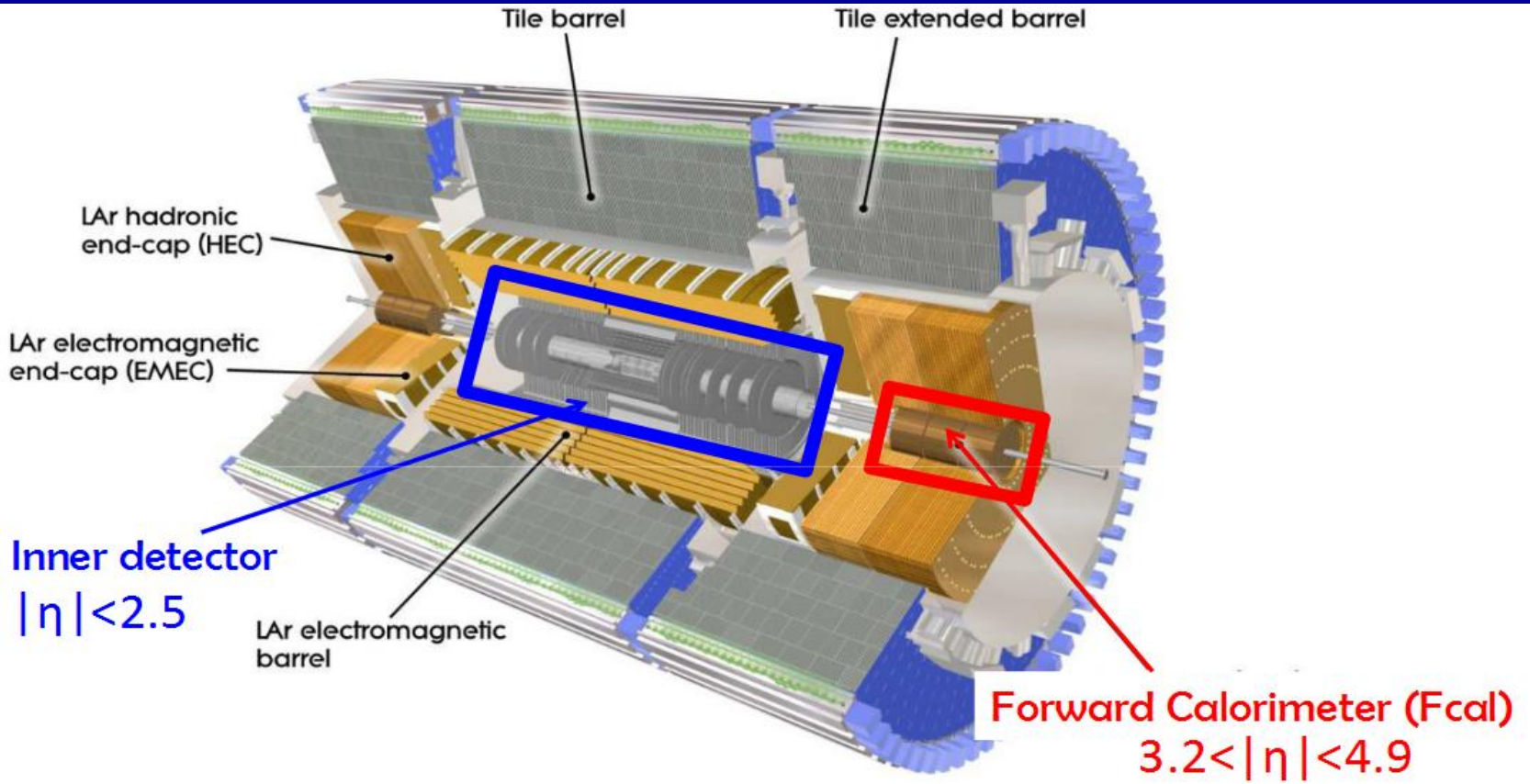


- Analysis uses charged particle tracks in the Inner Detector (ID) for constructing correlation functions.
- 'Event activity' characterization uses tracks reconstructed in the ID or the total energy in the forward calorimeter (FCal) on Pb-going side.
- Benefits from dedicated triggers implemented using the ATLAS L1 and HLT systems to enhance the number of high multiplicity events selected.

# ‘Event activity’ selection

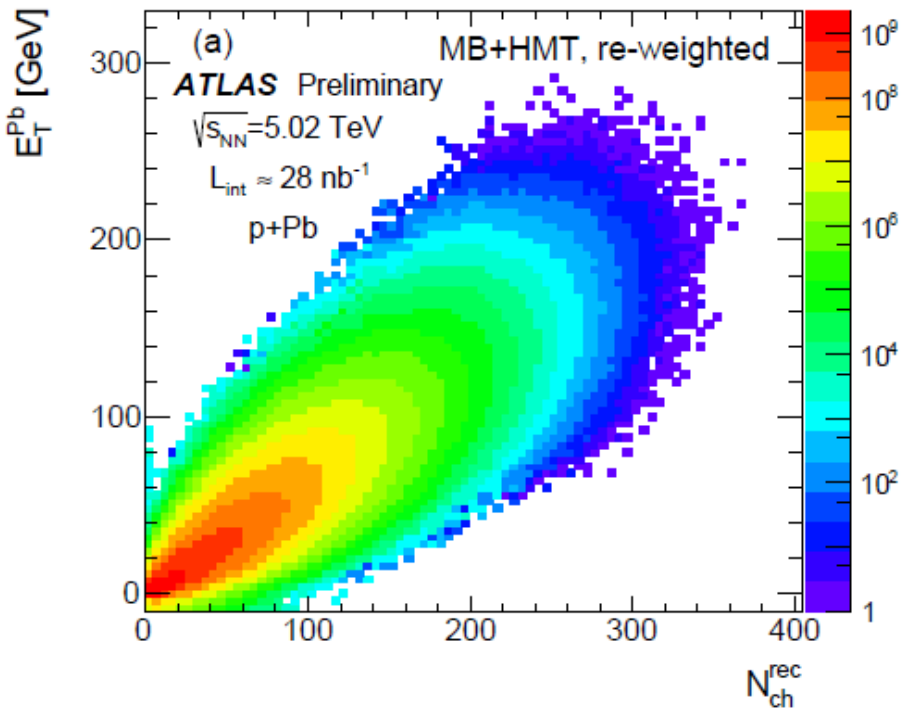


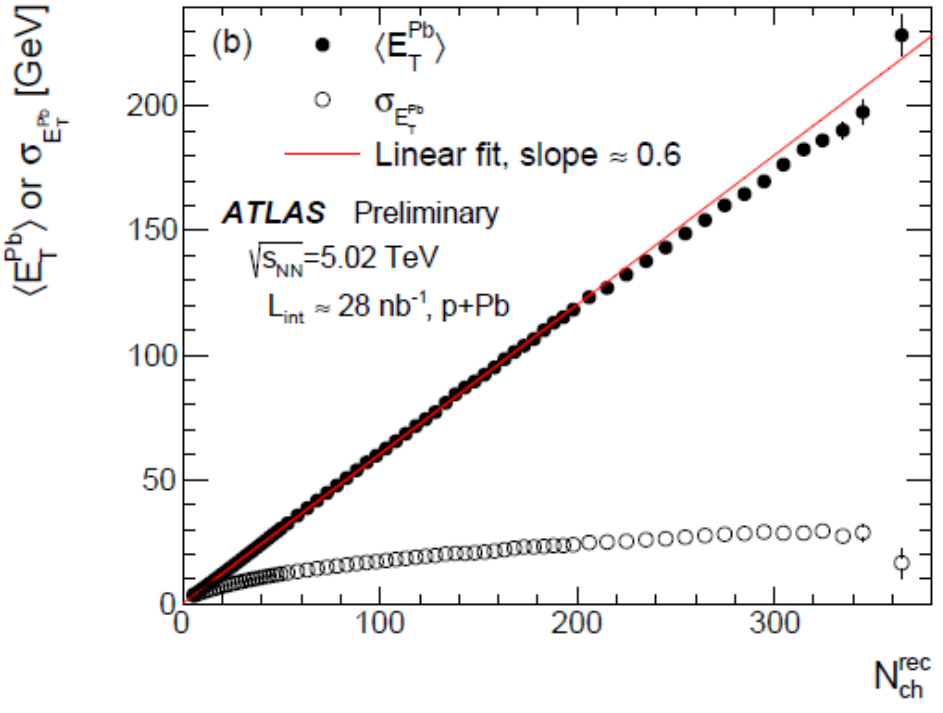


- Events are binned into several ‘event activity’ bins.
- Event activity → Characterized using:
  - $N_{ch}{}^{rec}$ : Number of charged particles with $p_T$ > 0.4 GeV in the ID
  - $E_T{}^{Pb}$ : Total transverse energy on the FCal on Pb-going side ..
- Events with low values of $N_{ch}{}^{rec}$ or $E_T{}^{Pb}$ are called ‘peripheral’ and those with high values are called ‘central’

# 2PC Analysis – recoil subtraction

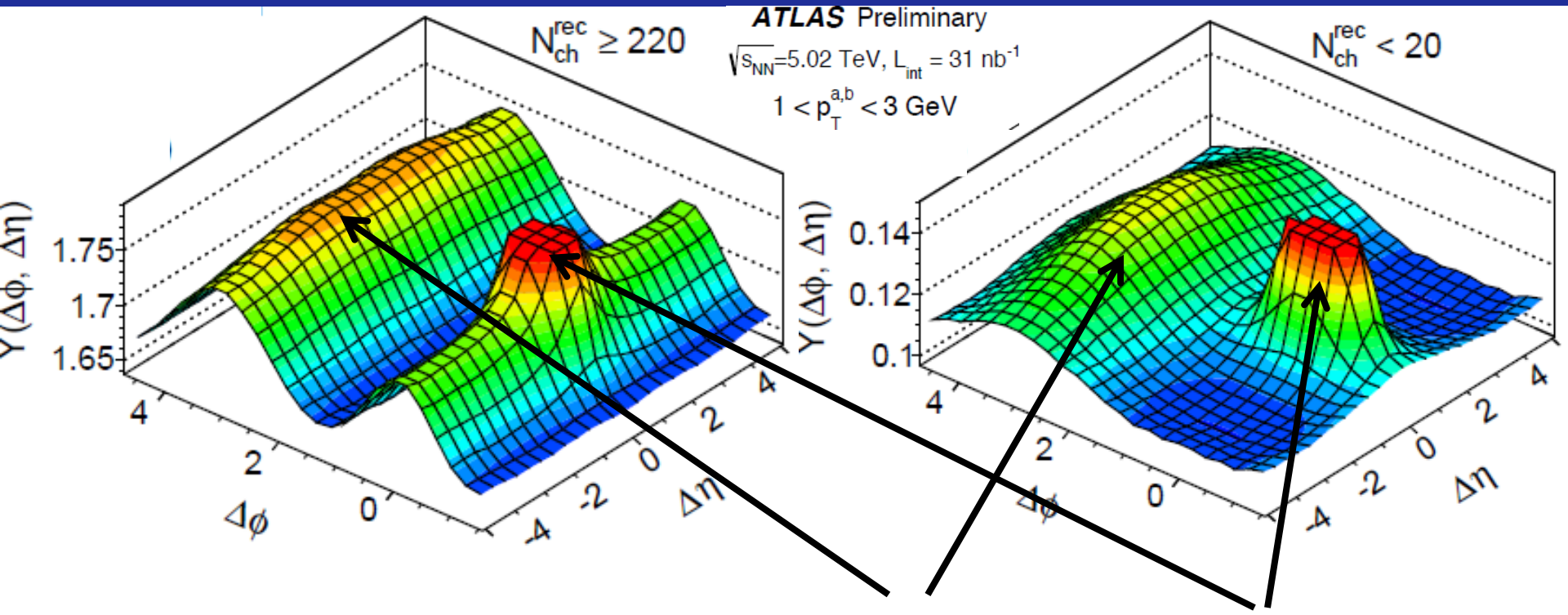


$$Y(\Delta\phi,\Delta\eta) = Y_{Ridge}(\Delta\phi) + Y_A(\Delta\phi,\Delta\eta) + Y_N(\Delta\phi,\Delta\eta)$$

Signal of interest — Away-side recoil — Near-side jet peak

- Jet peak & recoil in central collisions are estimated from the peripheral collisions and subtracted.

# 2PC Analysis – recoil subtraction

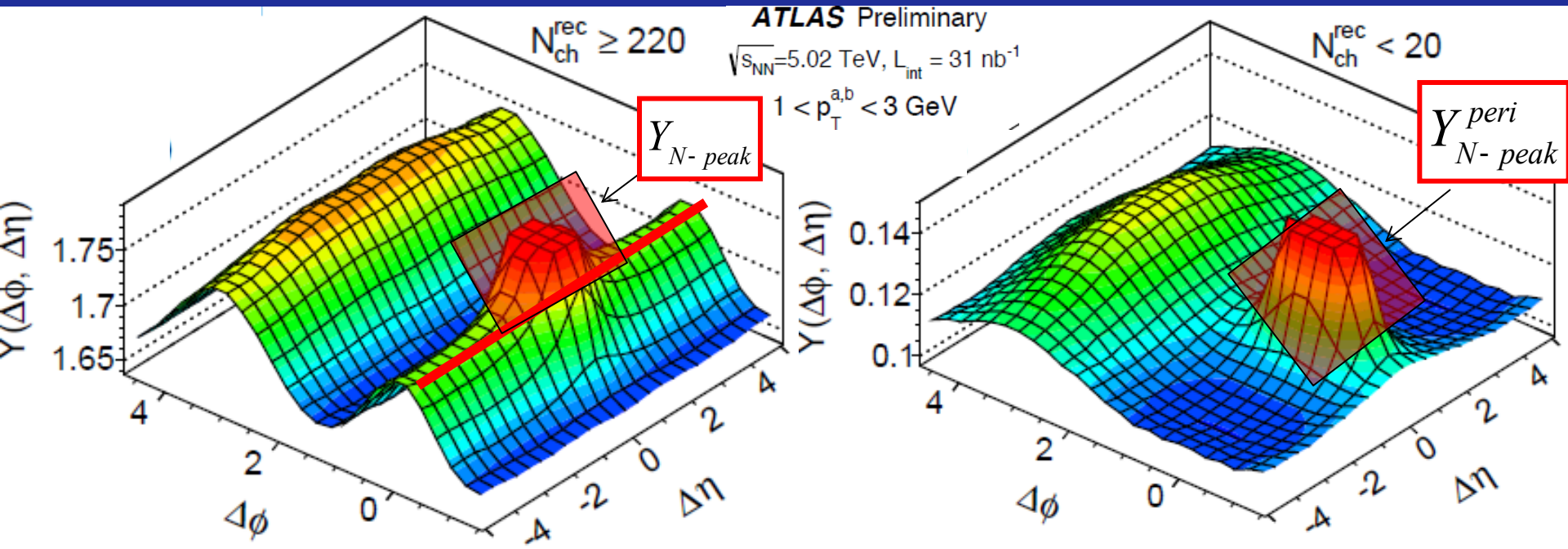


$$Y^{\mathrm{corr}}(\Delta\phi,\Delta\eta) = \frac{\int B(\Delta\phi,\Delta\eta)d\Delta\phi d\Delta\eta}{\pi\eta_{\Delta}^{\max}}\left(\frac{S(\Delta\phi,\Delta\eta)}{B(\Delta\phi,\Delta\eta)} - b_{\mathrm{ZYAM}}\right)$$

per-trigger yield in 2D

combinatorial background $b_{ZYAM}$

$$Y^{\mathrm{sub}}(\Delta\phi,\Delta\eta) = Y(\Delta\phi,\Delta\eta) - \alpha Y^{\mathrm{corr}}_{\mathrm{peri}}(\Delta\phi,\Delta\eta)$$

**α** is chosen such that

$$aY^{peri}_{N\text{-}peak} = Y_{N\text{-}peak}$$

$$Y^{\mathrm{N-Peak}} = \int_{|\Delta\eta|<1} Y(\Delta\eta)d\Delta\eta - \frac{1}{3}\int_{2<|\Delta\eta|<5} Y(\Delta\eta)d\Delta\eta$$

# 2PC Analysis – recoil subtraction

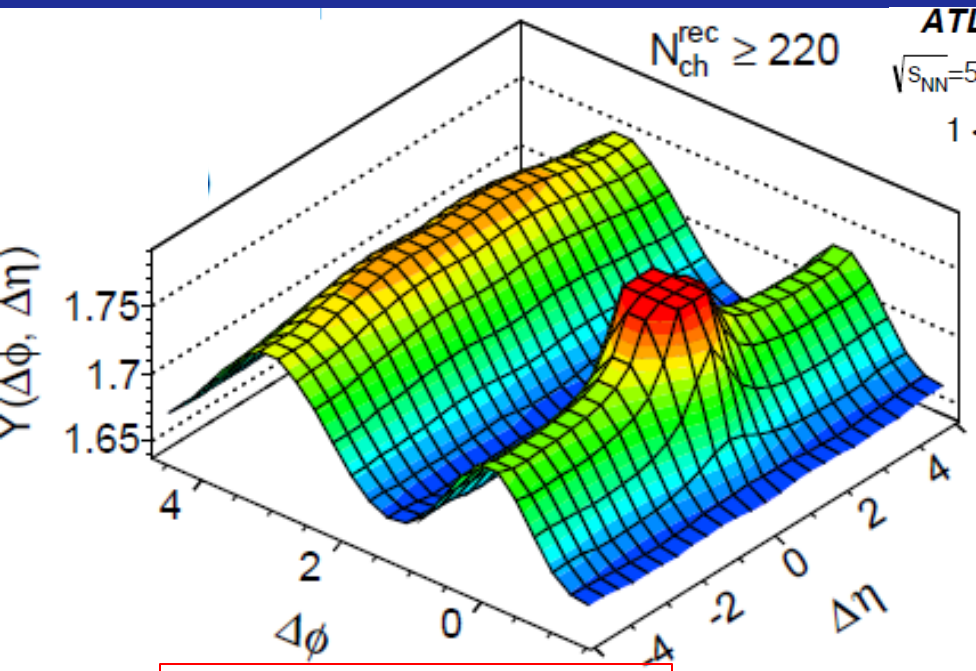


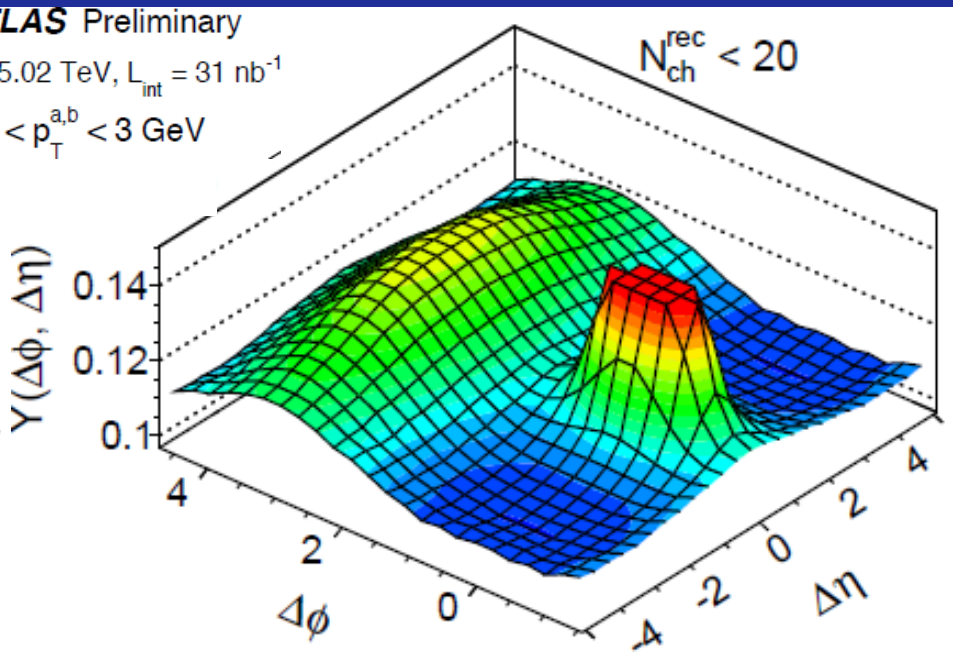


Before subtraction

After subtraction

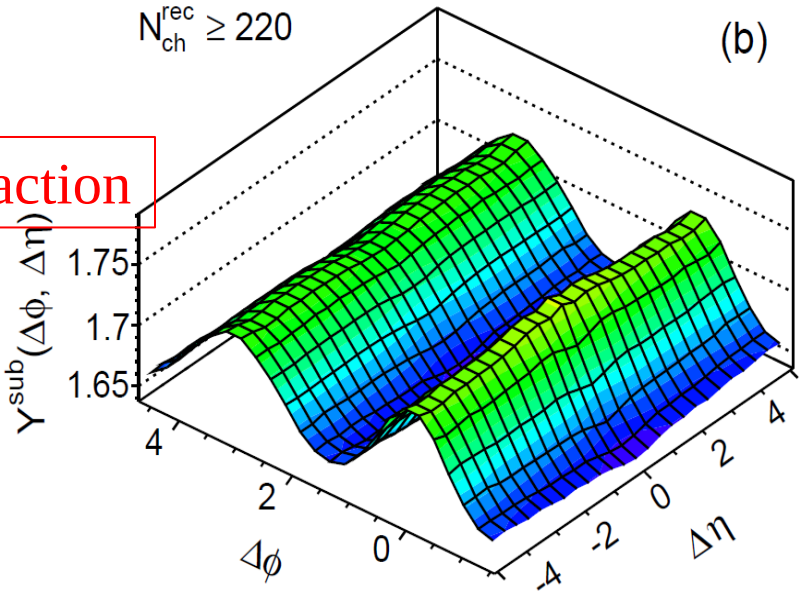


$$Y^{\mathrm{sub}}(\Delta\phi, \Delta\eta) = Y(\Delta\phi, \Delta\eta) - \alpha Y^{\mathrm{corr}}_{\mathrm{peri}}(\Delta\phi, \Delta\eta)$$

# Ridge at higher $p_T$

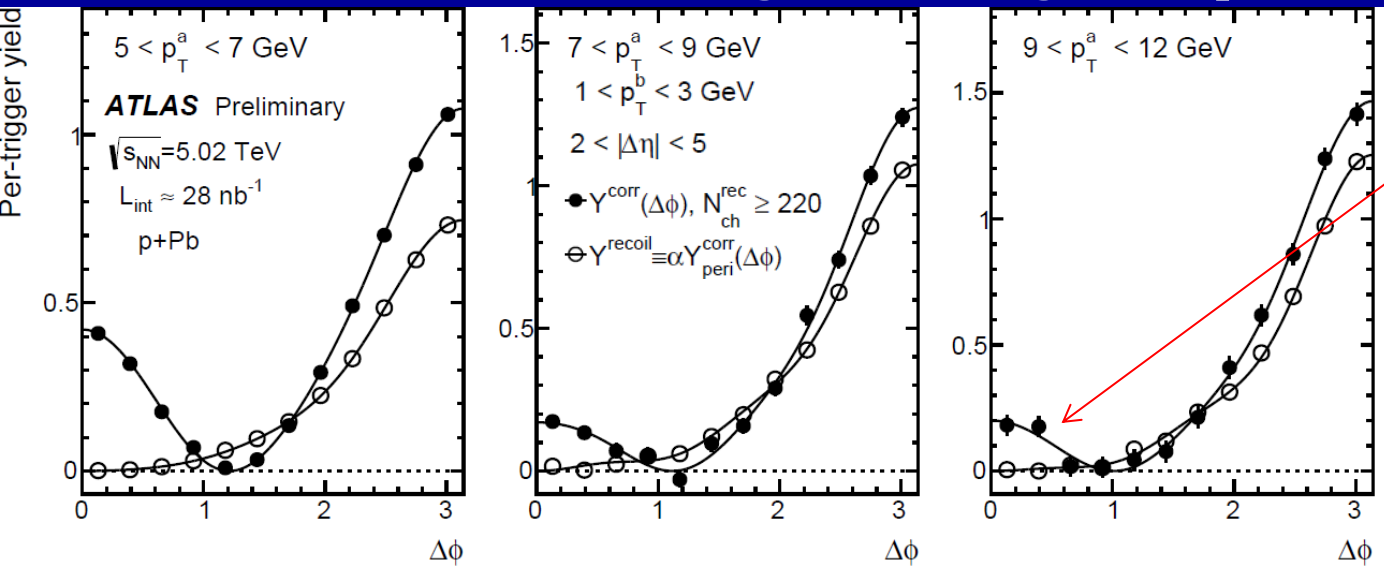


$$Y^{corr}(\Delta\phi) = \frac{\int B(\Delta\phi)d\Delta\phi}{\pi}\left(\frac{S(\Delta\phi)}{B(\Delta\phi)} - b_{ZYAm}\right)$$

- Near-side ridge visible through the entire $p_T$ range studied.
- Yield on away-side also larger than recoil component.

# Ridge at higher $p_T$

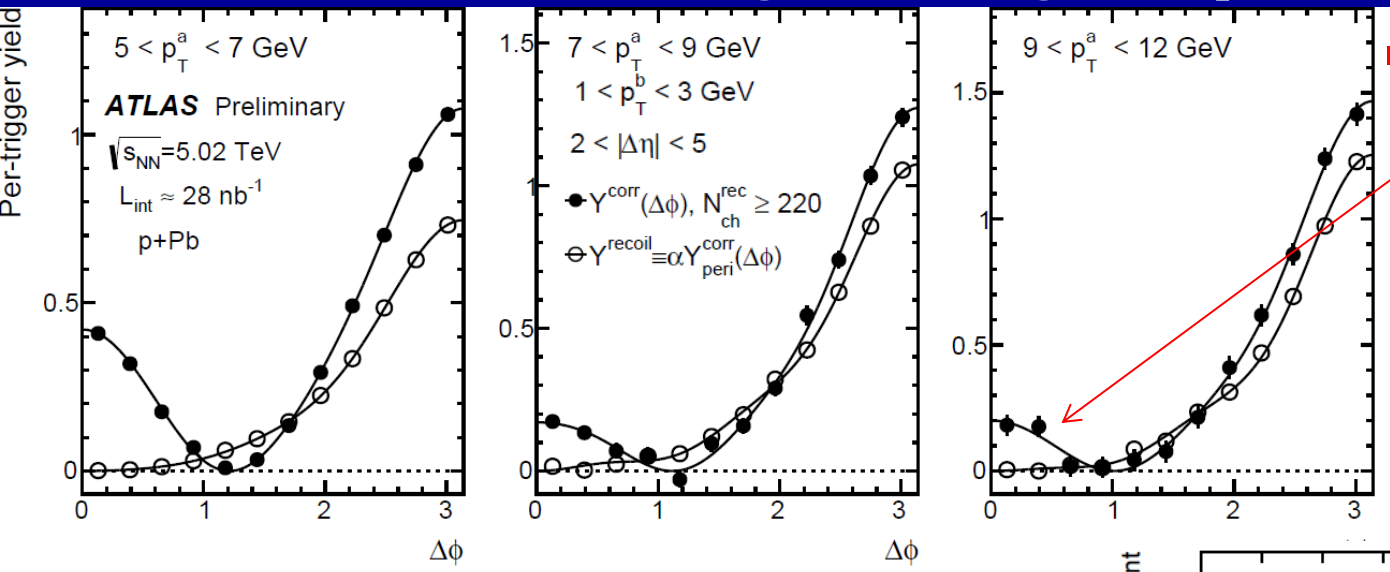


- Near-side ridge visible through the entire $p_T$ range studied.

$$Y^{corr}(\Delta\phi) = \frac{\int B(\Delta\phi)d\Delta\phi}{\pi}\left(\frac{S(\Delta\phi)}{B(\Delta\phi)} - b_{ZYAm}\right)$$

- Integrated yield on near-side:
  - increase with $p_T$
  - reaches maximum ~ 3 -- 4 GeV and then decreases.

$$Y_{int} = \int_a^b Y^{corr}(\Delta\phi)\, d\Delta\phi$$

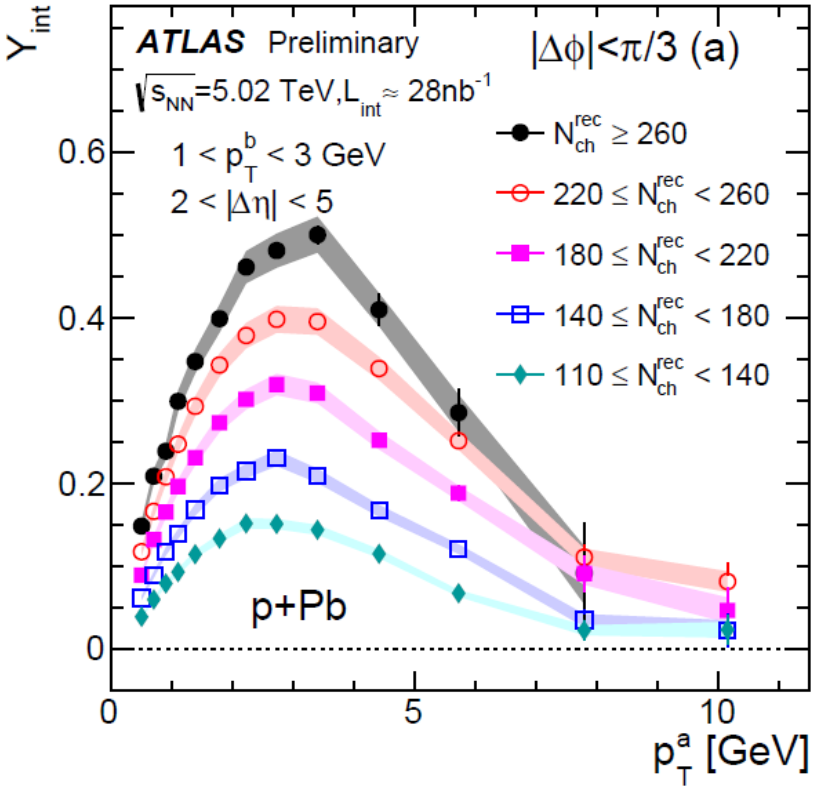

# Away side – Near side

- 2nd 3rd and 4th order harmonics cancel in the difference.
  - Yield from recoil matches the yield difference for $1 < {p_T}^b < 3$ GeV
  - Holds irrespective of ${p_T}^a$
- At other ${p_T}^b$, differences are seen
  - attributed to long range $v_1$.
- Similar observation as function of ${E_T}^{Pb}$

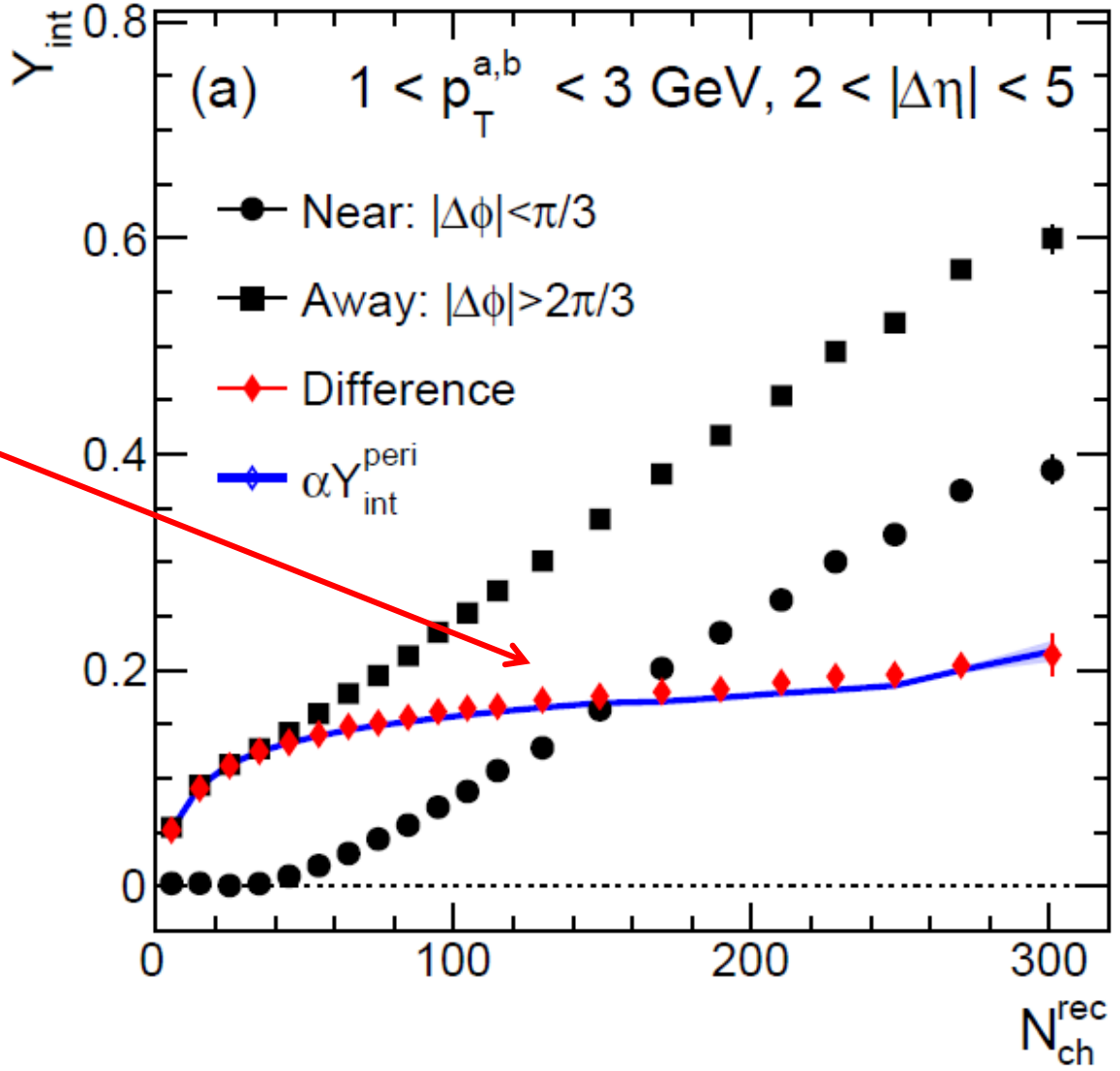


$$Y_{int} = \int_a^b Y^{corr}(\Delta\phi)\, d\Delta\phi$$

# $v_n$ vs $p_T$ before and after subtraction

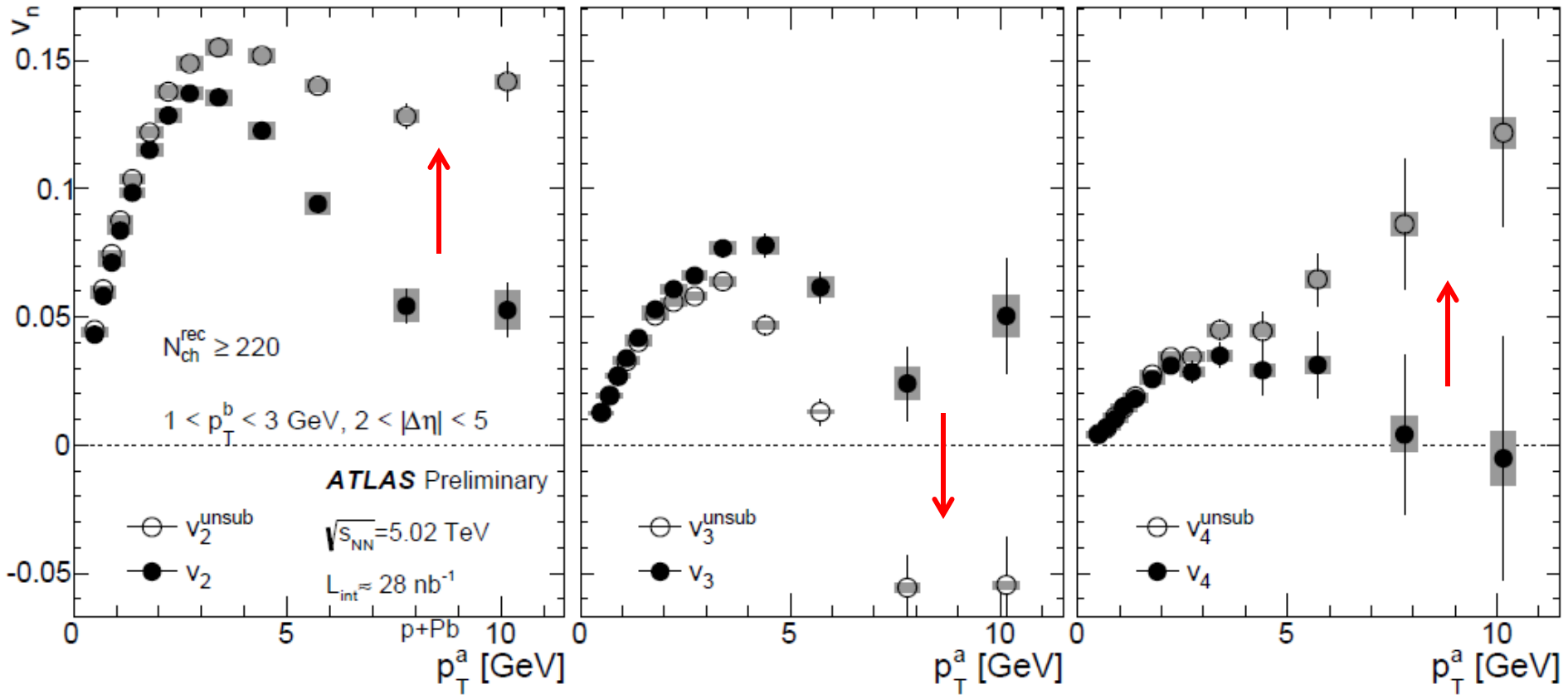


$$Y^{sub}(\Delta\phi) \sim 1 + \sum_n 2v_{n,n}\cos(n\Delta\phi)\ , \qquad v_n(p_T{}^a) = \frac{v_{n,n}(p_T{}^a, p_T{}^b)}{\sqrt{v_{n,n}(p_T{}^b, p_T{}^b)}}$$

- Bias in un subtracted values from recoil component.
  - Increases even harmonics
  - Decreases odd harmonics
- Subtracted values remain positive, throughout the $p_T$ range.

# $v_n$ vs $p_T$ for different n

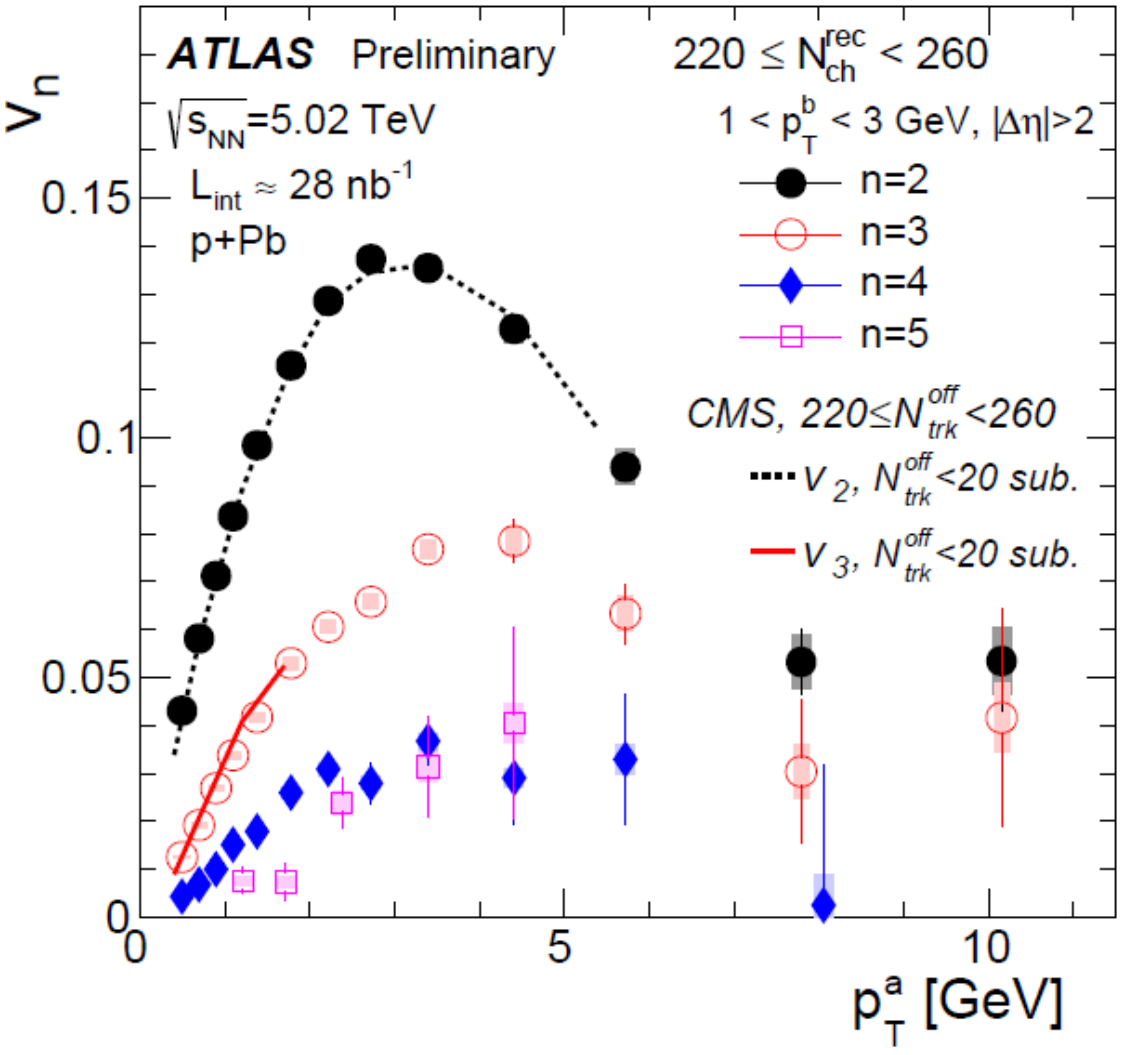


- $v_n$ decrease with increasing n.
- Rise with $p_T$ at low $p_T$ and then decraese.
- Non-zero $v_5$ in high multiplicity event classes.

# $v_n$ factorization

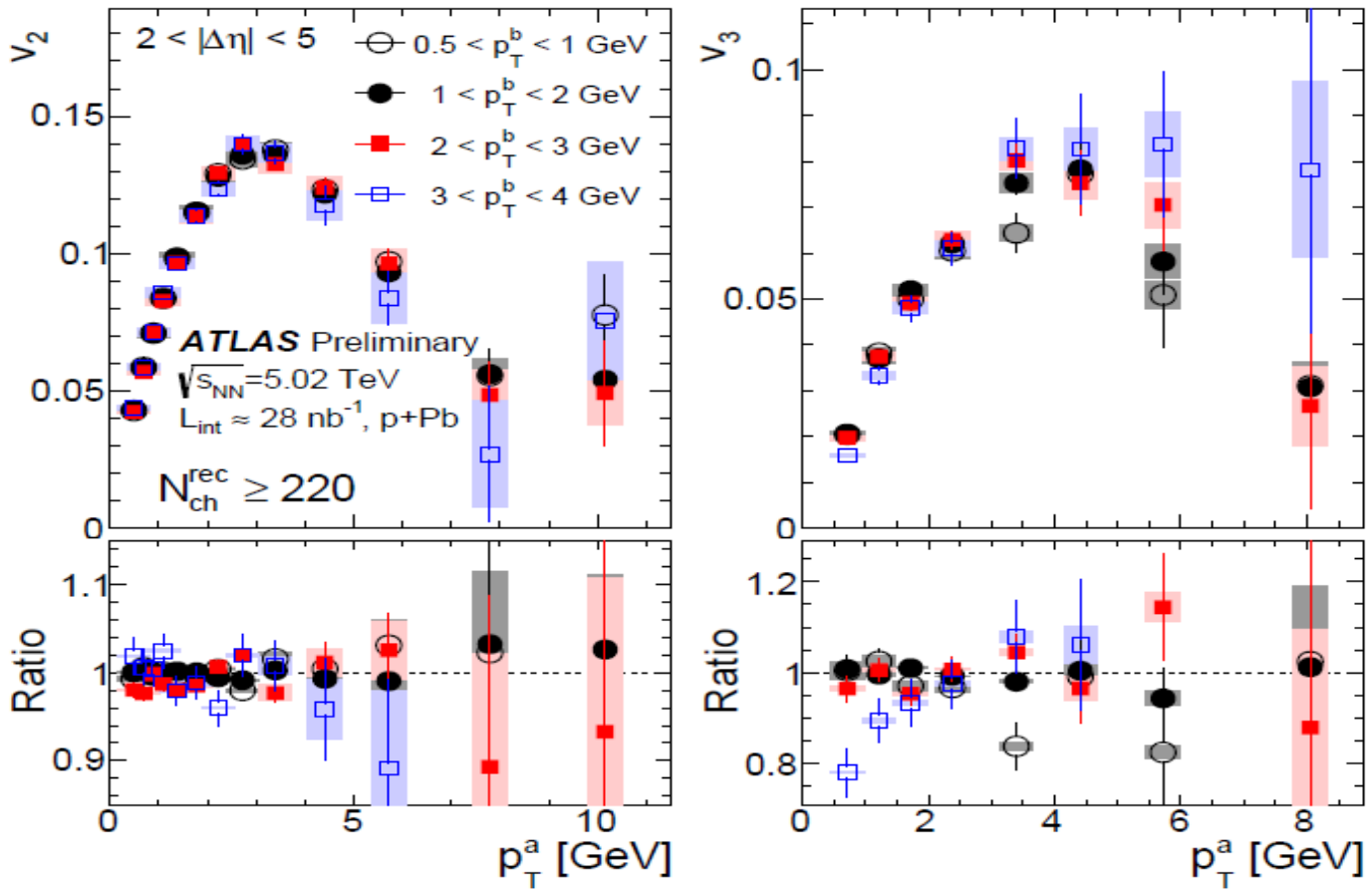


Check factorization assumption: $v_n(p_T{}^a) = \frac{v_{n,n}(p_T{}^a, p_T{}^b)}{\sqrt{v_{n,n}(p_T{}^b, p_T{}^b)}}$

- Good factorization seen for $v_2$ and $v_3$, particularly at low $p_T$, suggesting a global anisotropy.
  - Factorization holds within 4% for $v_2 < 4$ GeV and for $v_3 < 3$ GeV.

# $v_n$: Event activity dependence



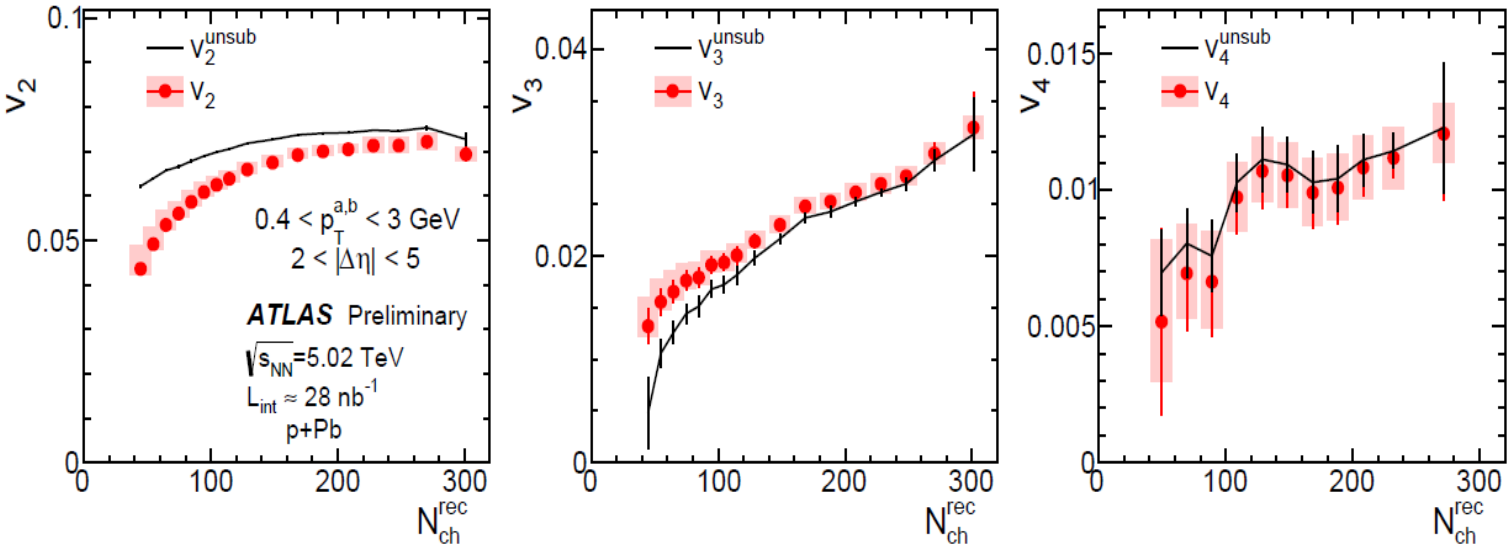


- $v_2$ show less variation for $N_{ch}^{rec}$>150, while $v_3$ continue to increase
- Recoil contribution does not affect the $v_n$ for large $N_{ch}^{rec}$, but significant deviations see for smaller $N_{ch}^{rec}$

# $v_n$: Event activity dependence



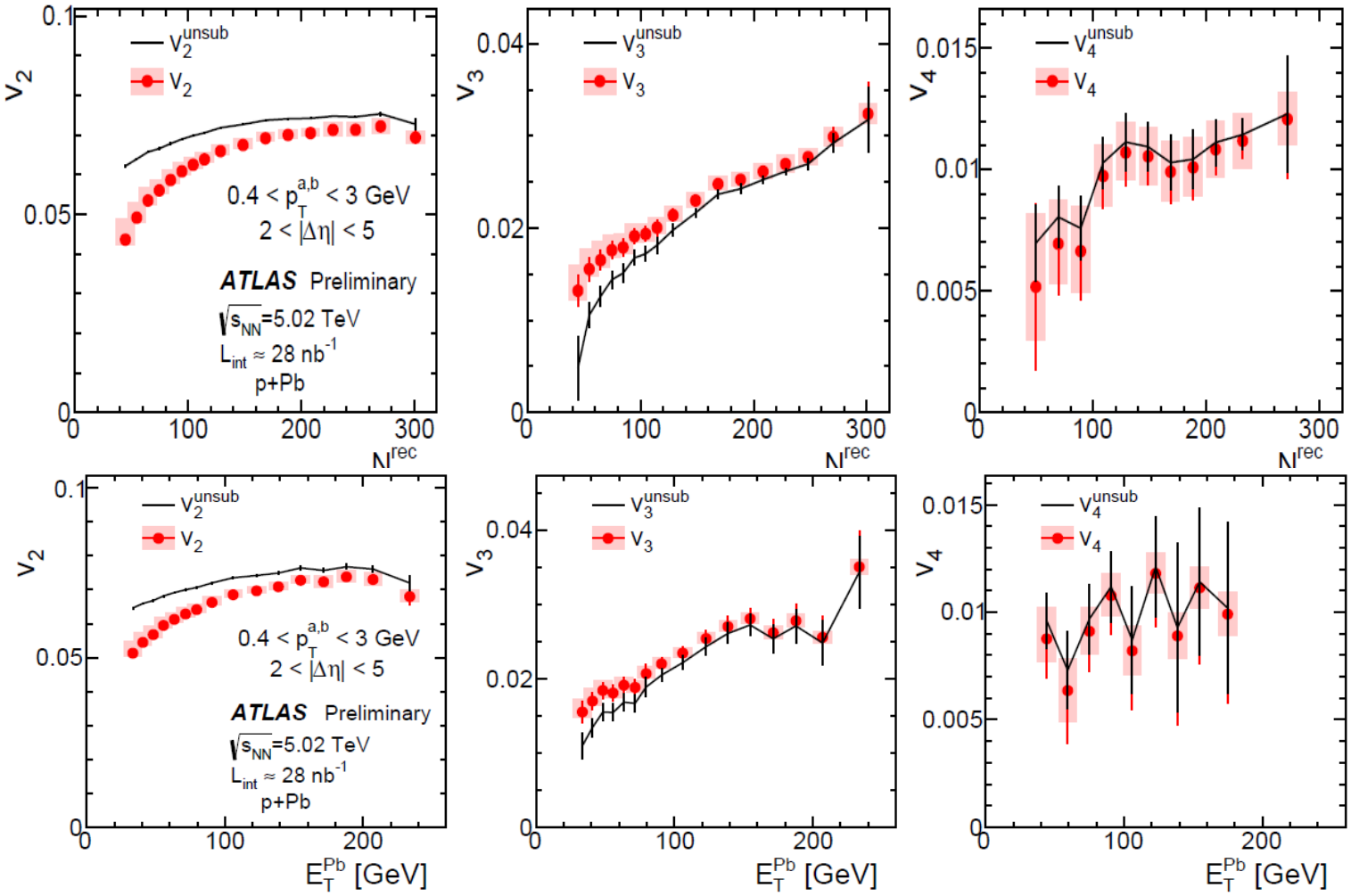


Similar behavior seen for $E_T^{Pb}$ dependence

- $v_2$ show less variation for $N_{ch}^{rec}$>150, while $v_3$ continue to increase
- Recoil contribution does not affect the $v_n$ for large $N_{ch}^{rec}$, but significant deviations see for smaller $N_{ch}^{rec}$

# Mapping $N_{ch}^{rec}$-dependence to $E_T^{Pb}$ dependence

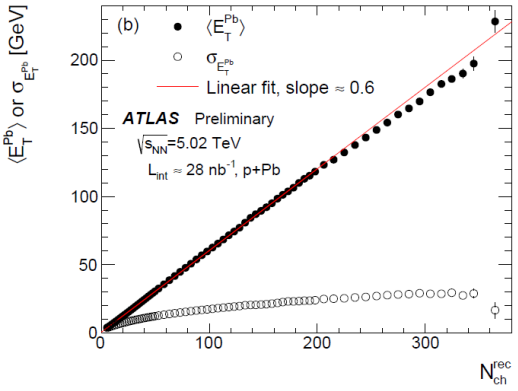


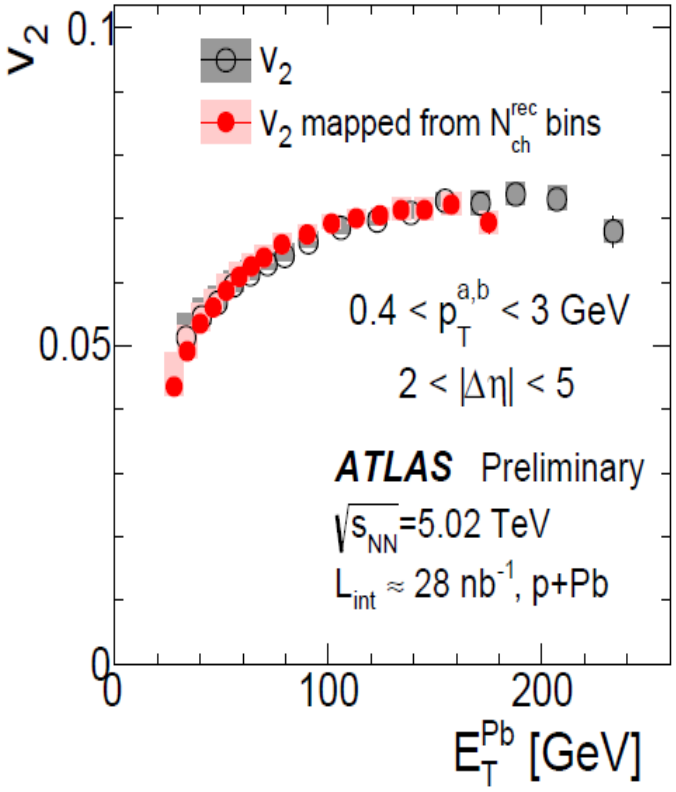


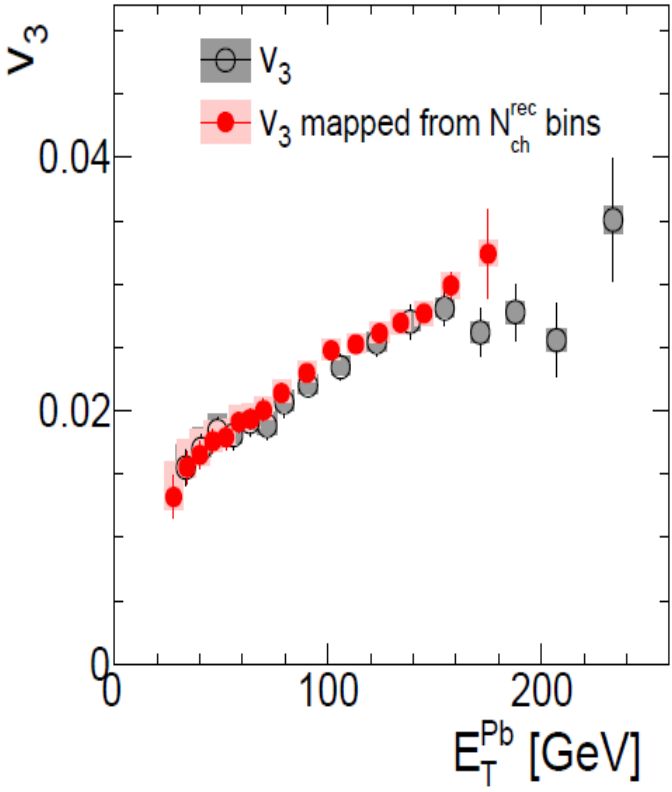


- The $v_n$ values for $N_{ch}^{rec}$ is plotted at corresponding $\langle E_T^{Pb} \rangle$ value, using the $N_{ch}^{rec}$ vs $E_T^{Pb}$ correlation data.
- Good consistency suggest that two event-activity definition captures the same azimuthal anisotropy of the long-range correlation.

# $v_{1,1}$ - First order harmonic in p+Pb

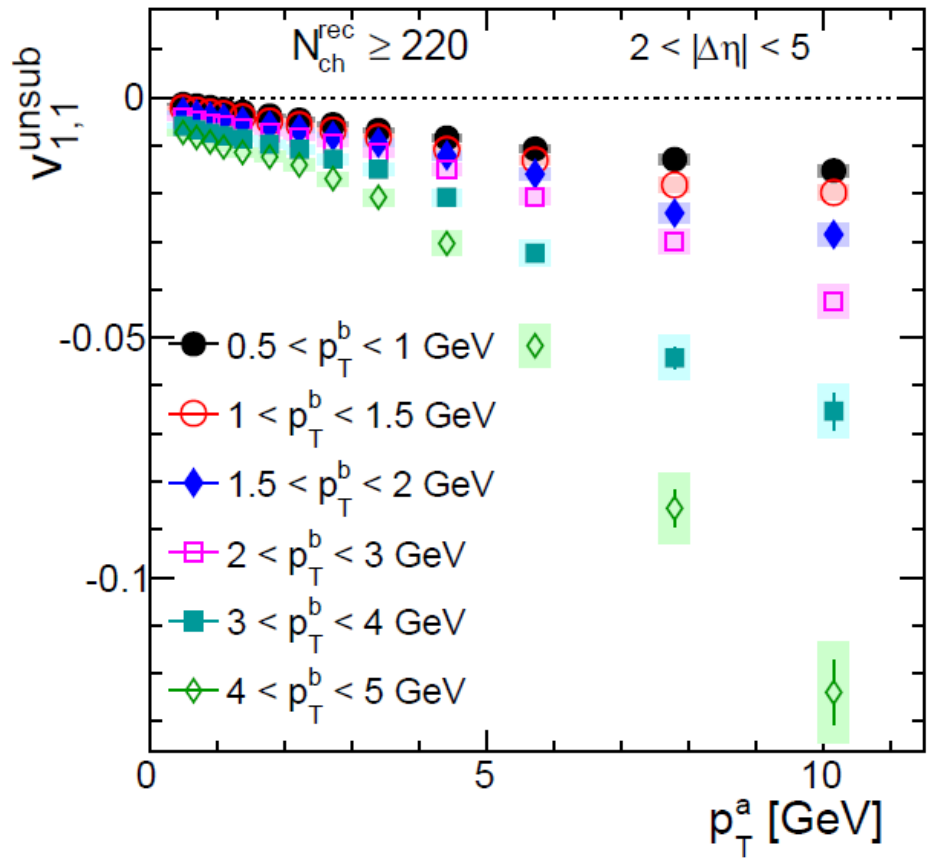


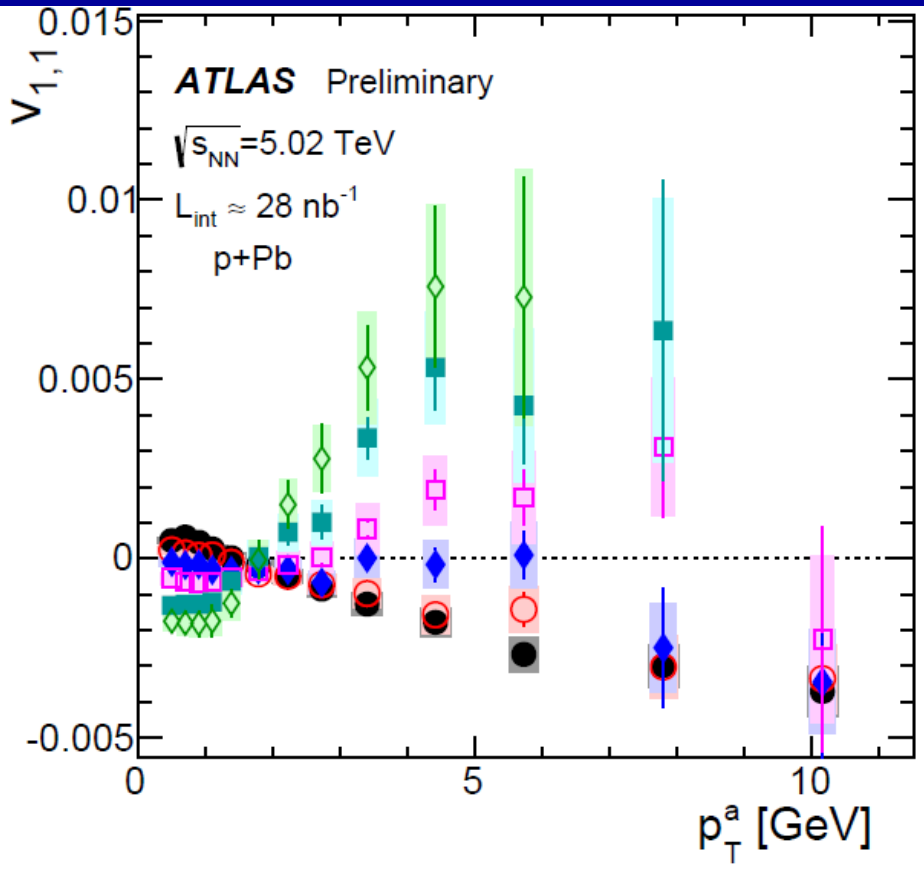


- Before recoil subtraction show mostly a linear dependence on $p_T{}^a$ .
- After recoil subtraction, a characteristic $p_T{}^{a,b}$ dependence
  - Similar to that seen in central Pb+Pb collisions
  - Attributed to long-range $v_1$ from density fluctuations which is –ve at low $p_T$ and +ve at higher $p_T$.

# Dipolar flow in p + Pb

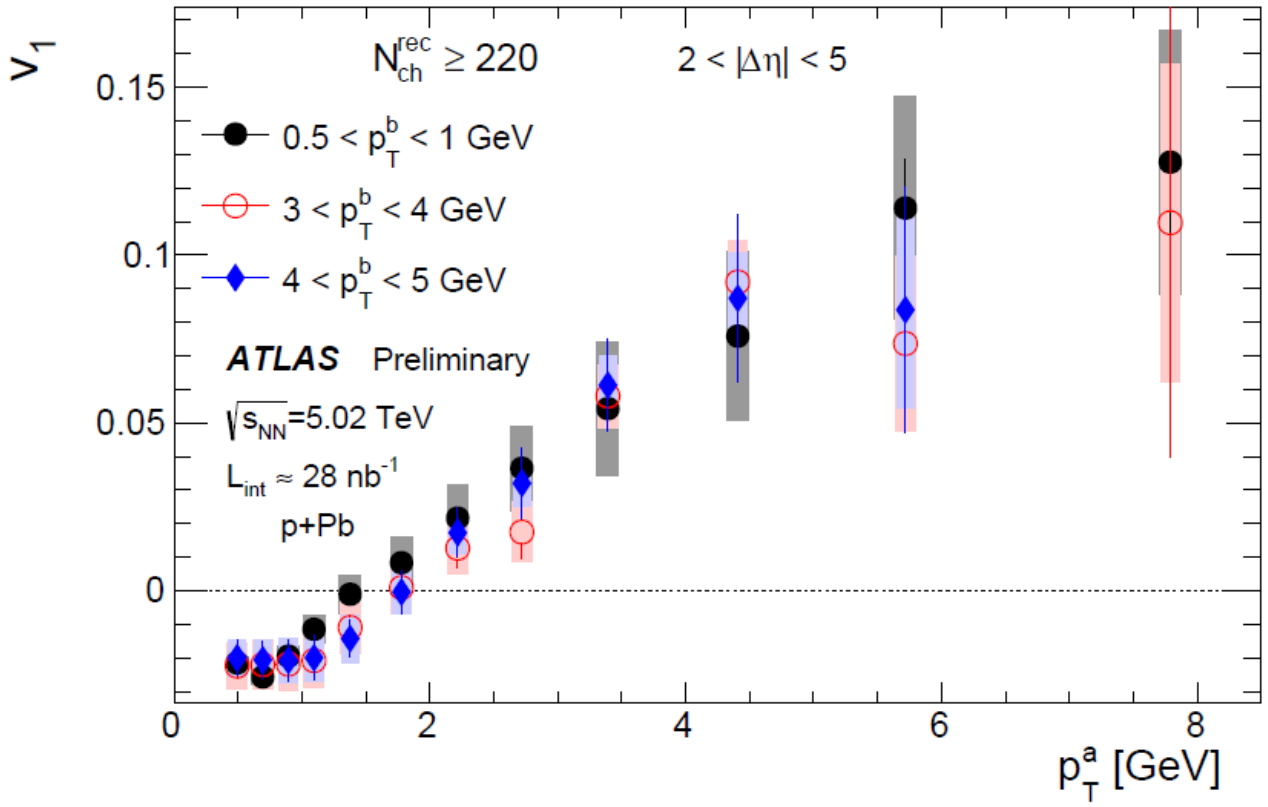


- Employ similar factorization as other harmonics, but account for sign change
- $v_{1,1}$ can be factorized as $v_1(p_T) \equiv \dfrac{v_{1,1}(p_T, p_T^{ref})}{v_1(p_T^{ref})}$

$$v_1(p_T^{ref}) = \text{sign}(p_T - p_T^0)\sqrt{|v_{1,1}(p_T^{ref}, p_T^{ref})|} \qquad p_T^0 = 1.5 \text{ GeV}$$

- Good agreement, suggesting a single particle modulation.

# Comparison of $v_n$ in p+Pb and peripheral Pb+Pb.

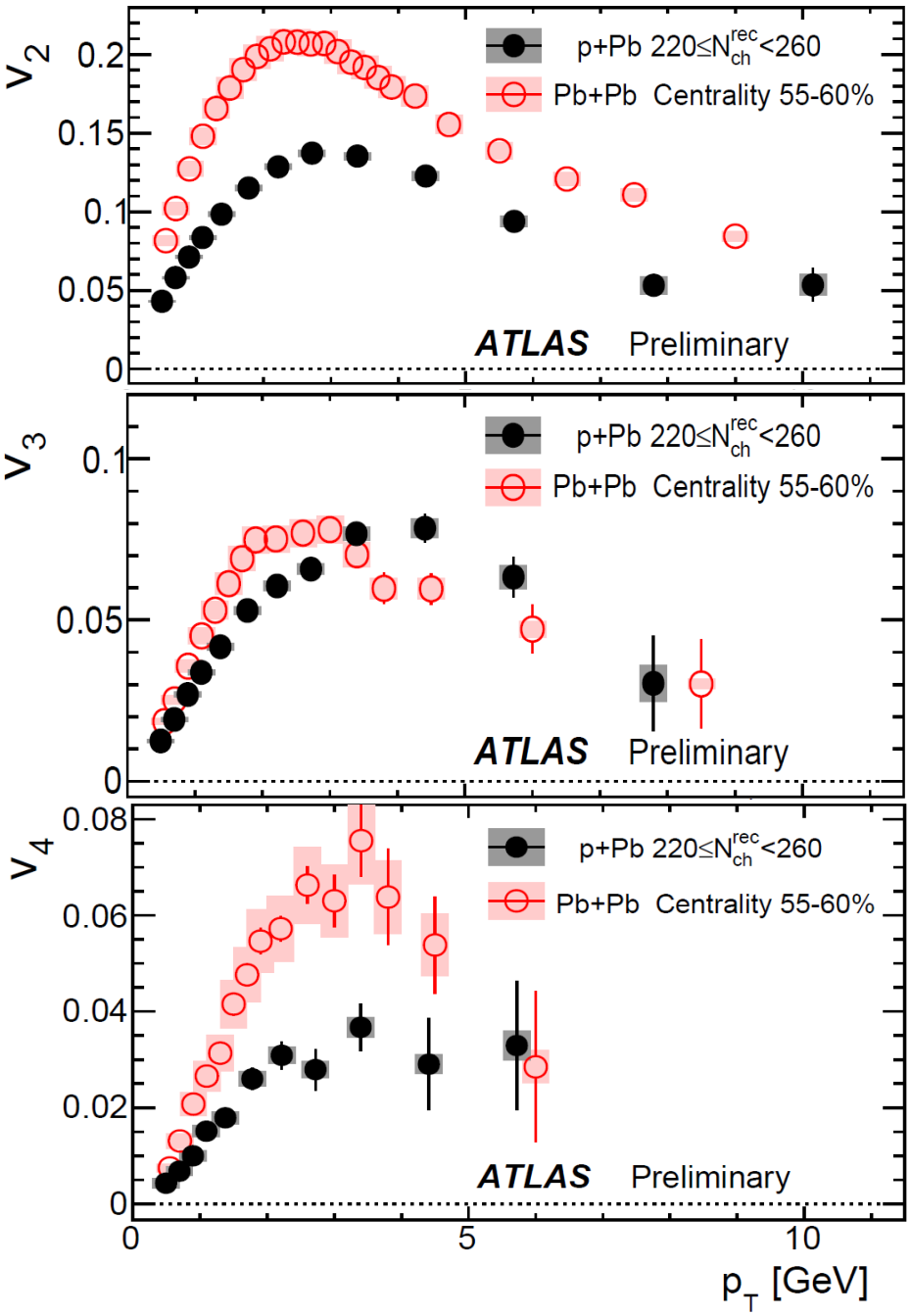


- Significantly larger $v_2$ and $v_4$ in Pb+Pb, but comparable magnitudes for $v_3$!
  - Large elliptic geometry from overlap in PbPb
  - $v_4$ and $v_2$ are coupled

  $v_4 = \sqrt{{c_0}^2 + {c_1}^2 {v_2}^4}$ (see talk by Soumya)

- Compare $v_n\,(p_T)_{p+Pb}$ with $v_n\,(p_T/K)_{Pb+Pb}$, *(Teaney et.al arXiv:1312.6770 [nucl-th].)*
  - K=1.25, ratio of $\langle p_T \rangle$.

- p+Pb: $\langle N_{ch} \rangle \pm \sigma = 259 \pm 13$
- Pb+Pb: $\langle N_{ch} \rangle \pm \sigma = 241 \pm 43$

# $v_n$ scaling between the p+Pb and Pb+Pb systems.

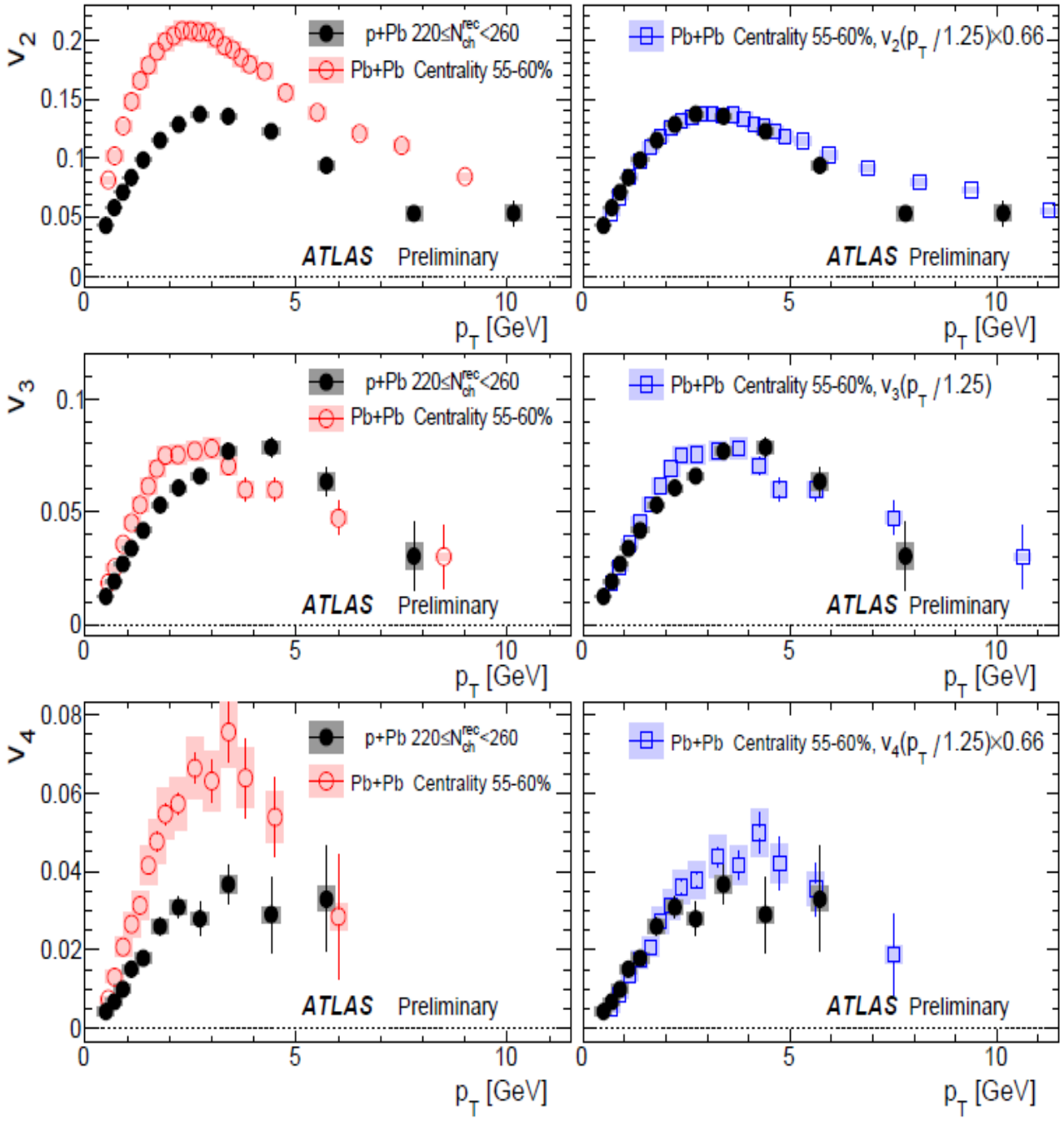


- $v_2$ values, after scaling the $p_T$ axis, differ only by a scale factor between the two systems.
- Suggests a similar origin for $v_2$ in the two systems and similar medium response to initial geometry?

# Summary and Conclusions

- The long-range correlation in high multiplicity events persists to $p_T$ ~ 12 GeV.

- $v_n$ vs $p_T$ and event-activity.
  - First 5 Fourier harmonics measured
  - The magnitude of $v_n$ decrease with increasing n.
  - $v_n$ found to increase with ${N_{ch}}^{rec}$ and ${E_T}^{Pb}$, but $v_2$ shows a saturation at higher event activity values.
  - The first order harmonic, $v_1$, is found to cross zero ~ 1.5-2.0 GeV and increases to ~0.1 for $p_T$ > 4 GeV.

- Comparison with peripheral Pb+Pb
  - $v_n(p_T)$, n = 1,2,3, are compared between p+Pb and Pb+Pb collisions with similar multiplicity.
  - Similar shape in $p_T$ observed, once a scaling is applied to account for the difference in mean $p_T$ between the two systems.

# BACK UP

# Summary of systematic uncertainties

Summary of relative percentage uncertainties on PTY.

| | |
|---|---|
| Residual pair acceptance [%] | 1–2 |
| ZYAM procedure [%] | 0.2–1.5 |
| Tracking efficiency & material [%] | 4.2 |
| Residual pileup [%] | 0–2 |

Summary of relative percentage uncertainties on $v_n$.

| | $n=1$ | $n=2$ | $n=3$ | $n=4$ | $n=5$ |
|---|---|---|---|---|---|
| Residual pair acceptance [%] | 1–5 | <0.5 | 1–4 | 7–12 | 7–20 |
| ZYAM procedure [%] | 0.6 | 0.3 | 0.3 | 0.5 | 0.6 |
| Tracking efficiency& material [%] | 1 | 0.4 | 0.8 | 1.2 | 2.4 |
| Monte-Carlo closure [%] | 4 | 1 | 2 | 4 | 8 |
| Residual pileup [%] | 0–2 | 0–2 | 0–2 | 0–2 | 0–2 |
| Uncertainty on scale factor $\alpha$ [%] | 8–30 | 0.2–10 | 0.2–12 | 0.2–14 | 1–14 |
| Choice of peripheral events for $N_{\mathrm{ch}}^{\mathrm{rec}} > 160$ or $E_{\mathrm{T}}^{\mathrm{Pb}} > 100$ GeV [%] | 4 | 1 | 1 | 2 | 4 |

# High multiplicity triggers

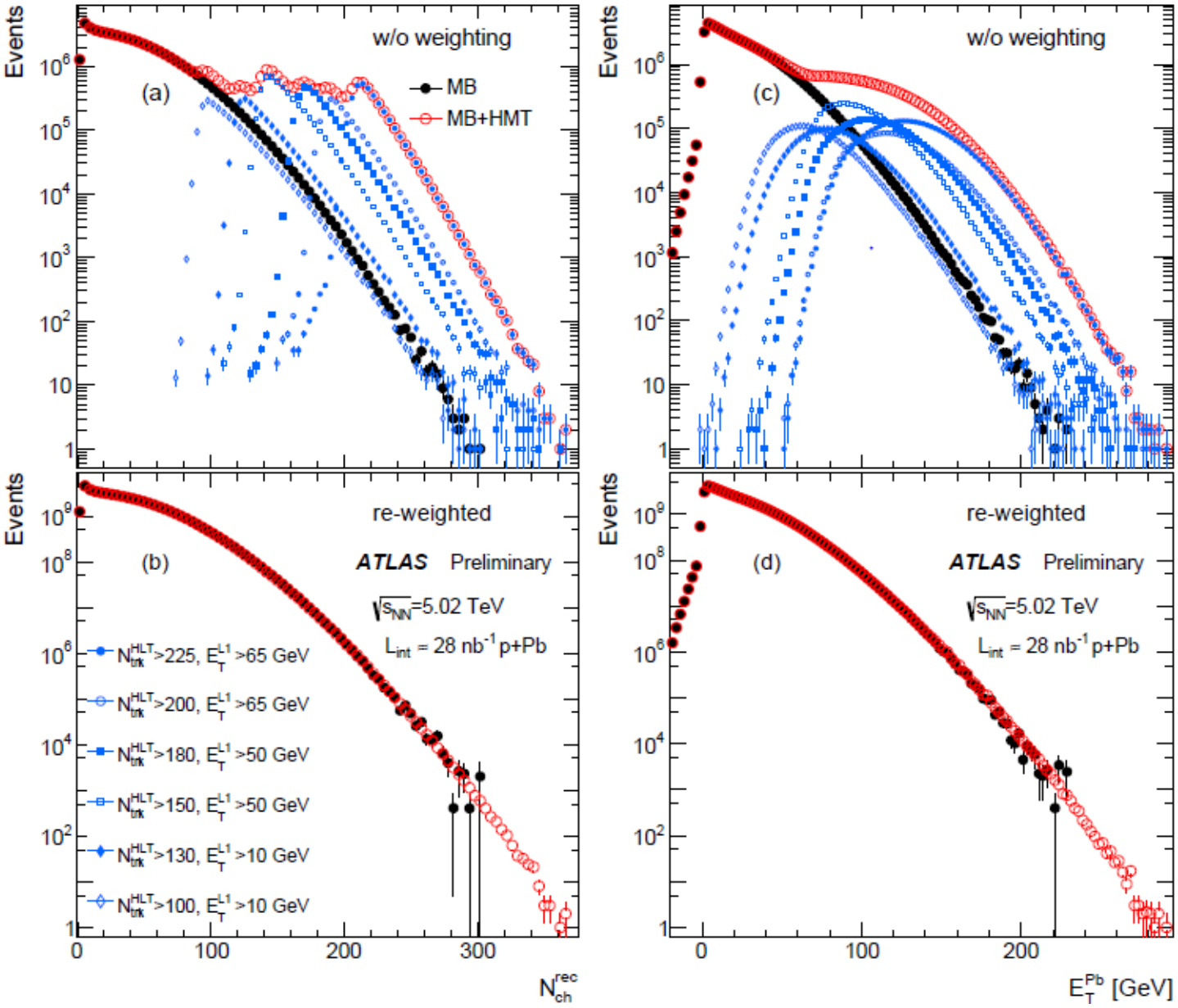


- Enhancement from individual HMT selection (top)
- Reweighted by MB+HMT distribution (bottom)
- Reweighting takes into account the prescale and trigger efficiency

# $N_{ch}^{rec} - E_T^{Pb}$ correlation for MB and MB+HMT

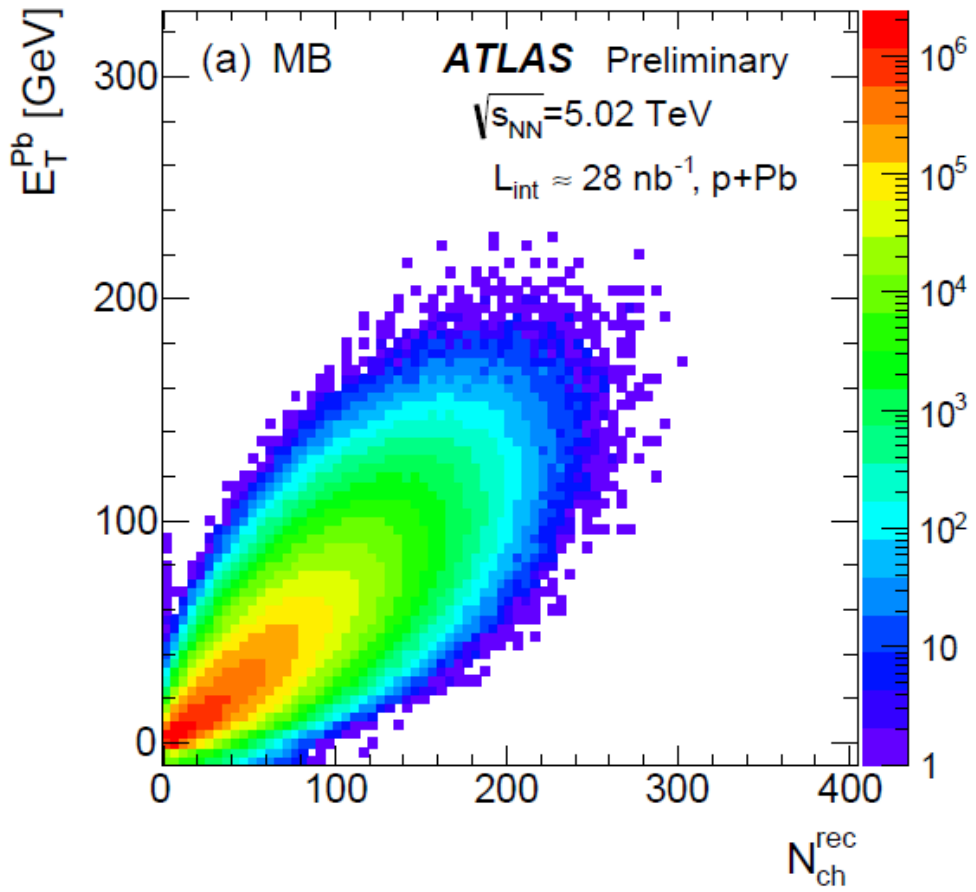


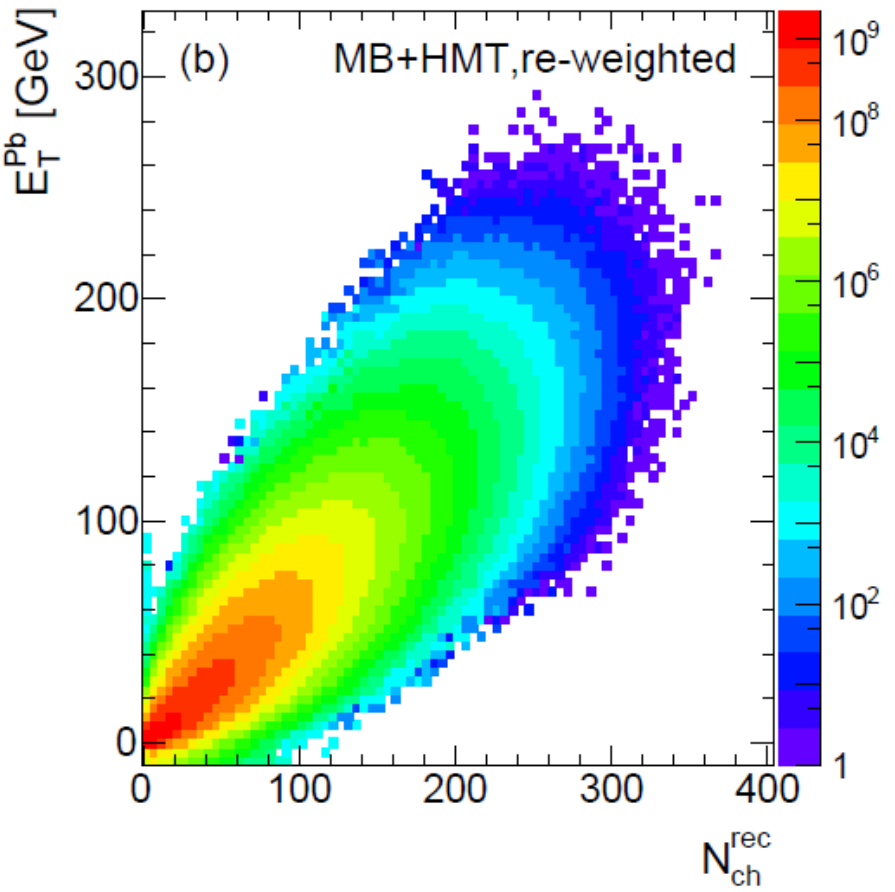

# Event activity classes

| Event-activity classes based on $N_{\mathrm{ch}}^{\mathrm{rec}}$ | | | | | Event-activity classes based on $E_{\mathrm{T}}^{\mathrm{Pb}}$ | | | | |
|---|---|---|---|---|---|---|---|---|---|
| $N_{\mathrm{ch}}^{\mathrm{rec}}$ range | fraction | $\langle E_{\mathrm{T}}^{\mathrm{Pb}} \rangle$ [GeV] | $\langle N_{\mathrm{ch}}^{\mathrm{rec}} \rangle$ | $\langle N_{\mathrm{ch}} \rangle$ | $E_{\mathrm{T}}^{\mathrm{Pb}}$ range [GeV] | fraction | $\langle E_{\mathrm{T}}^{\mathrm{Pb}} \rangle$ [GeV] | $\langle N_{\mathrm{ch}}^{\mathrm{rec}} \rangle$ | $\langle N_{\mathrm{ch}} \rangle$ |
| $[0, 40)$ | 0.58 | 12.5 | 19.0 | $24.4 \pm 1.1$ | $< 25$ | 0.59 | 10.2 | 21.7 | $28.0 \pm 1.3$ |
| $[40, 80)$ | 0.32 | 35.3 | 56.4 | $74.4 \pm 3.3$ | $[25, 50)$ | 0.27 | 35.1 | 54.7 | $72.2 \pm 3.3$ |
| $[80, 110)$ | 0.081 | 56.8 | 91.7 | $122 \pm 6$ | $[50, 75)$ | 0.096 | 61.5 | 81.4 | $108 \pm 5$ |
| $[110, 140)$ | 0.023 | 74.2 | 121 | $161 \pm 7$ | $[75, 100)$ | 0.025 | 84.5 | 106 | $141 \pm 6$ |
| $[140, 180)$ | 0.0053 | 93.0 | 153 | $203 \pm 9$ | $[100, 130)$ | 0.0051 | 110 | 130 | $173 \pm 8$ |
| $[180, 220)$ | $4.6 \times 10^{-4}$ | 116 | 192 | $255 \pm 12$ | $[130, 165)$ | $5.6 \times 10^{-4}$ | 141 | 156 | $208 \pm 9$ |
| $[220, 260)$ | $2.6 \times 10^{-5}$ | 136 | 231 | $307 \pm 14$ | $[165, 200)$ | $2.7 \times 10^{-5}$ | 174 | 186 | $248 \pm 11$ |
| $[260, 370)$ | $1.2 \times 10^{-6}$ | 158 | 271 | $361 \pm 16$ | $[200, 300)$ | $1.0 \times 10^{-6}$ | 208 | 214 | $284 \pm 13$ |

- Some of the event activity classes used in the analysis and the fraction of MB events in each class

# Analysis Overview – II : Recoil subtraction

- Use yield in peripheral event class to estimate contribution from away-side jet, momentum conservation etc (recoil component) (ATLAS 2012, ALICE 2012, ALICE 2013)

- A scale factor, α, is applied to take into account the increase of the near-side jet yield (CMS 2013)

$$\alpha = Y^{\mathrm{N-Peak}} / Y^{\mathrm{N-Peak}}_{\mathrm{peri}}$$

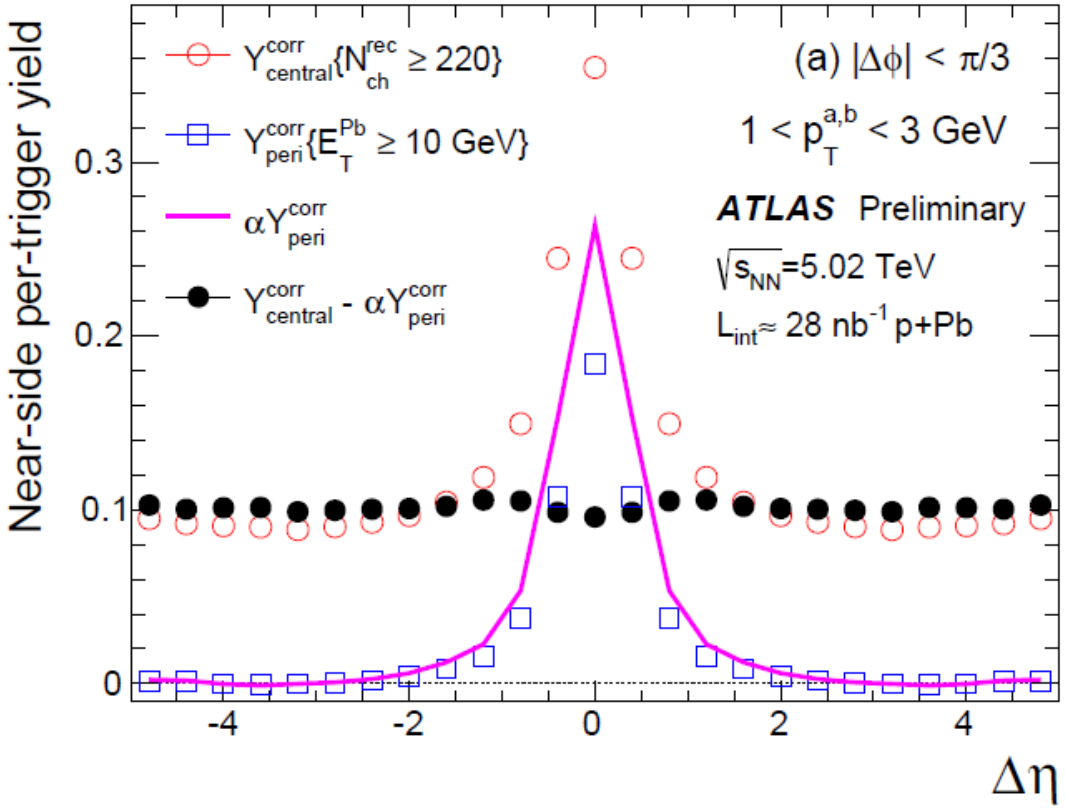


$$Y^{\mathrm{N-Peak}} = \int_{|\Delta\eta|<1} Y(\Delta\eta)d\Delta\eta - \frac{1}{3}\int_{2<|\Delta\eta|<5} Y(\Delta\eta)d\Delta\eta$$

where, $Y(\Delta\eta) = \int_{|\Delta\phi|<1} Y(\Delta\phi, \Delta\eta)\Delta\phi.$

- Stability of jet yield is evaluated by varying the Δη region used for long-range subtraction

# Analysis Overview – III

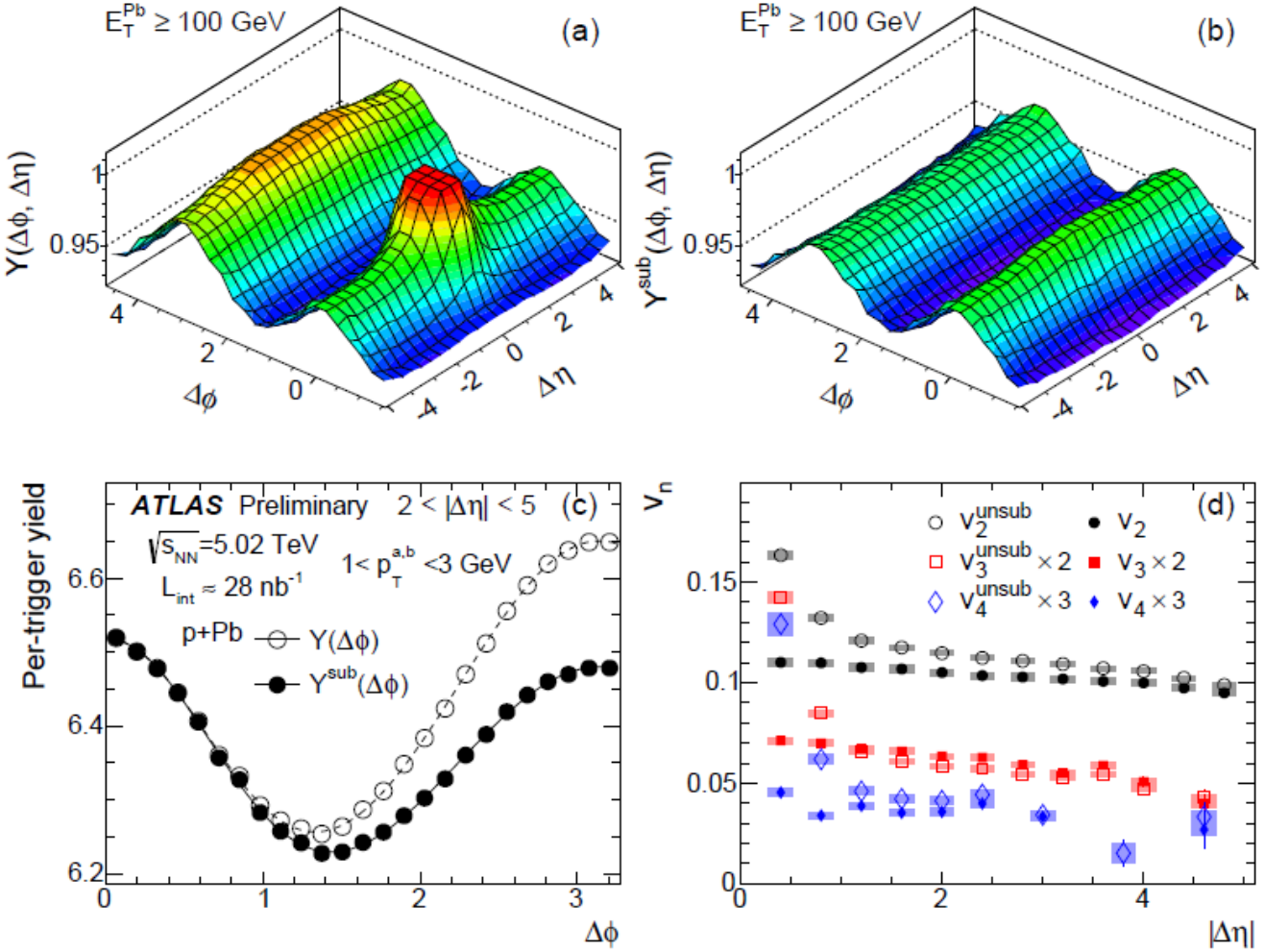


- Recoil subtracted distribution:,
- Fourier harmonics : $Y^{sub}(\Delta\phi) \sim 1 + \sum_n 2v_{n,n}\cos(n\Delta\phi)$
- Factorization: $v_n(p_T{}^a) = \frac{v_{n,n}(p_T{}^a, p_T{}^b)}{\sqrt{v_{n,n}(p_T{}^b, p_T{}^b)}}$,

$$Y(\Delta\phi) = \frac{\int B(\Delta\phi)d\Delta\phi}{\pi}\frac{S(\Delta\phi)}{B(\Delta\phi)}$$

- Fourier harmonics are also evaluated from the unsubtracted distribution, $Y(\Delta\phi)$, in a similar manner and are denoted by $v_{n,n}{}^{dir}$ and $v_n{}^{dir}$.

# Near side – Away side (II)

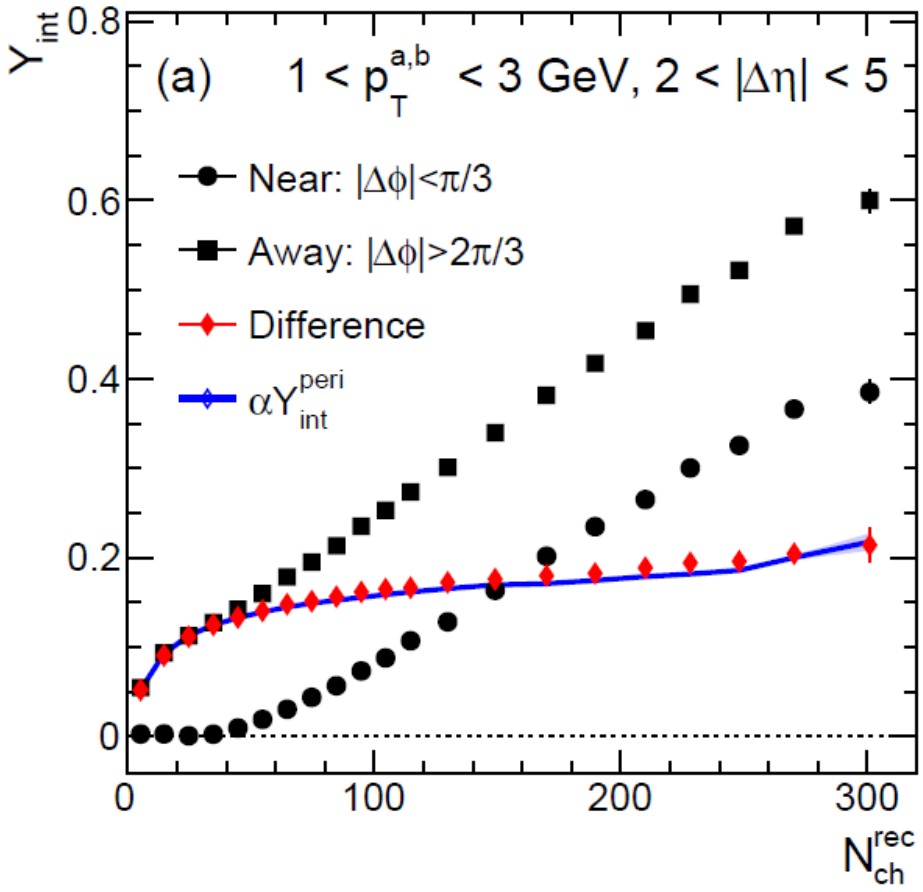


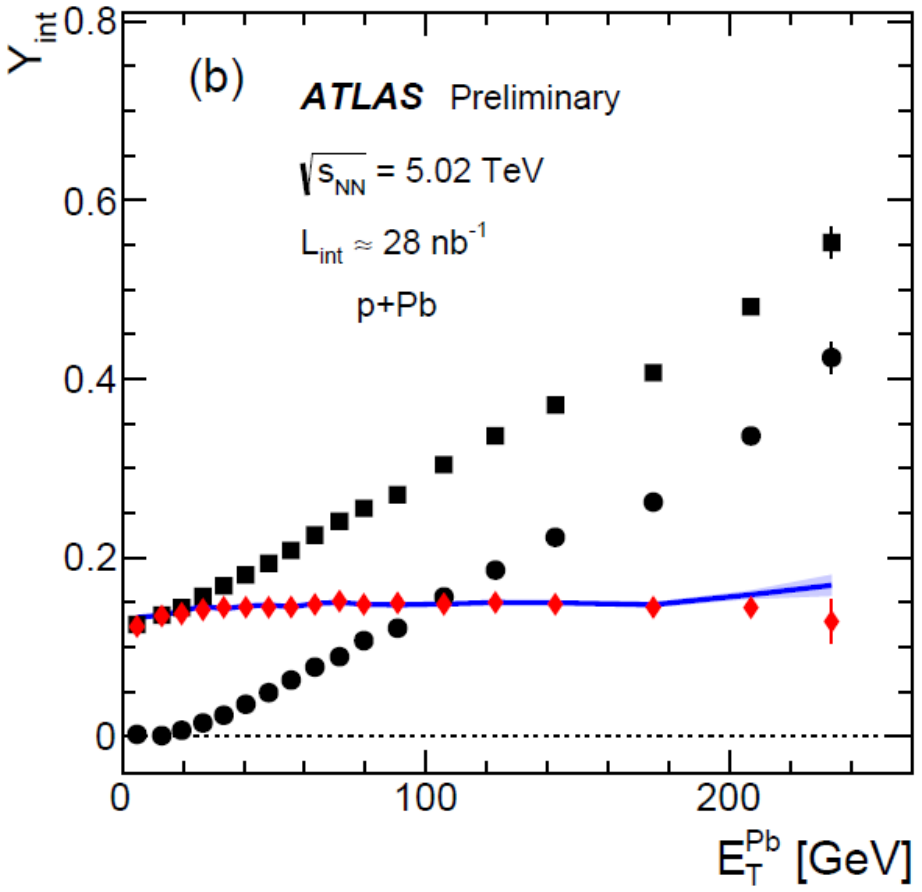


- Away side yield in ${E_T}^{Pb}$ < 10 GeV is ~ 2x that in ${N_{ch}}^{rec}$ < 20

# $v_1$ in different $N_{ch}{}^{rec}$ classes

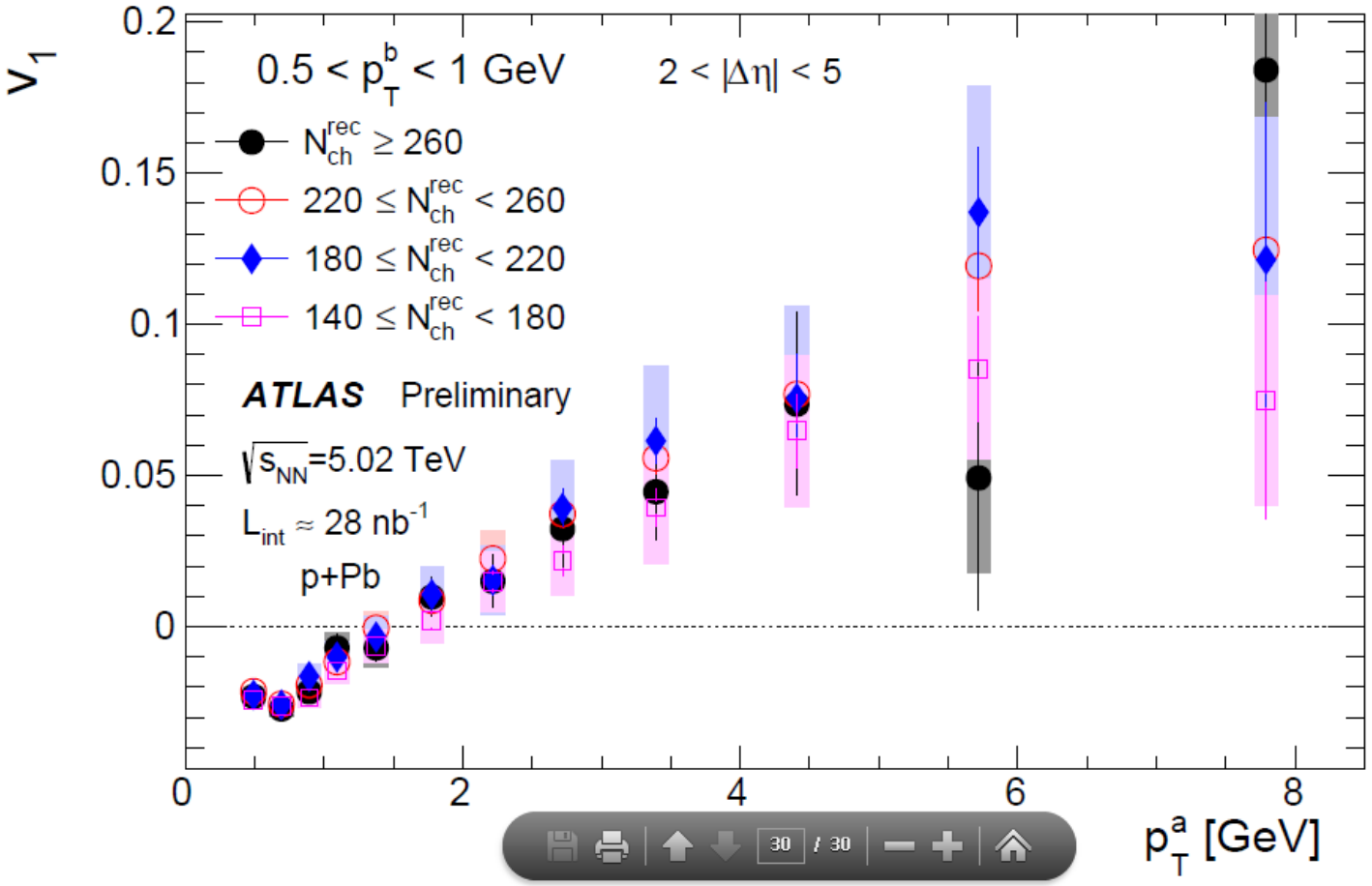


- Similar $p_T$ dependence in other event-activity classes as well.

# Dipolar flow in Pb+Pb

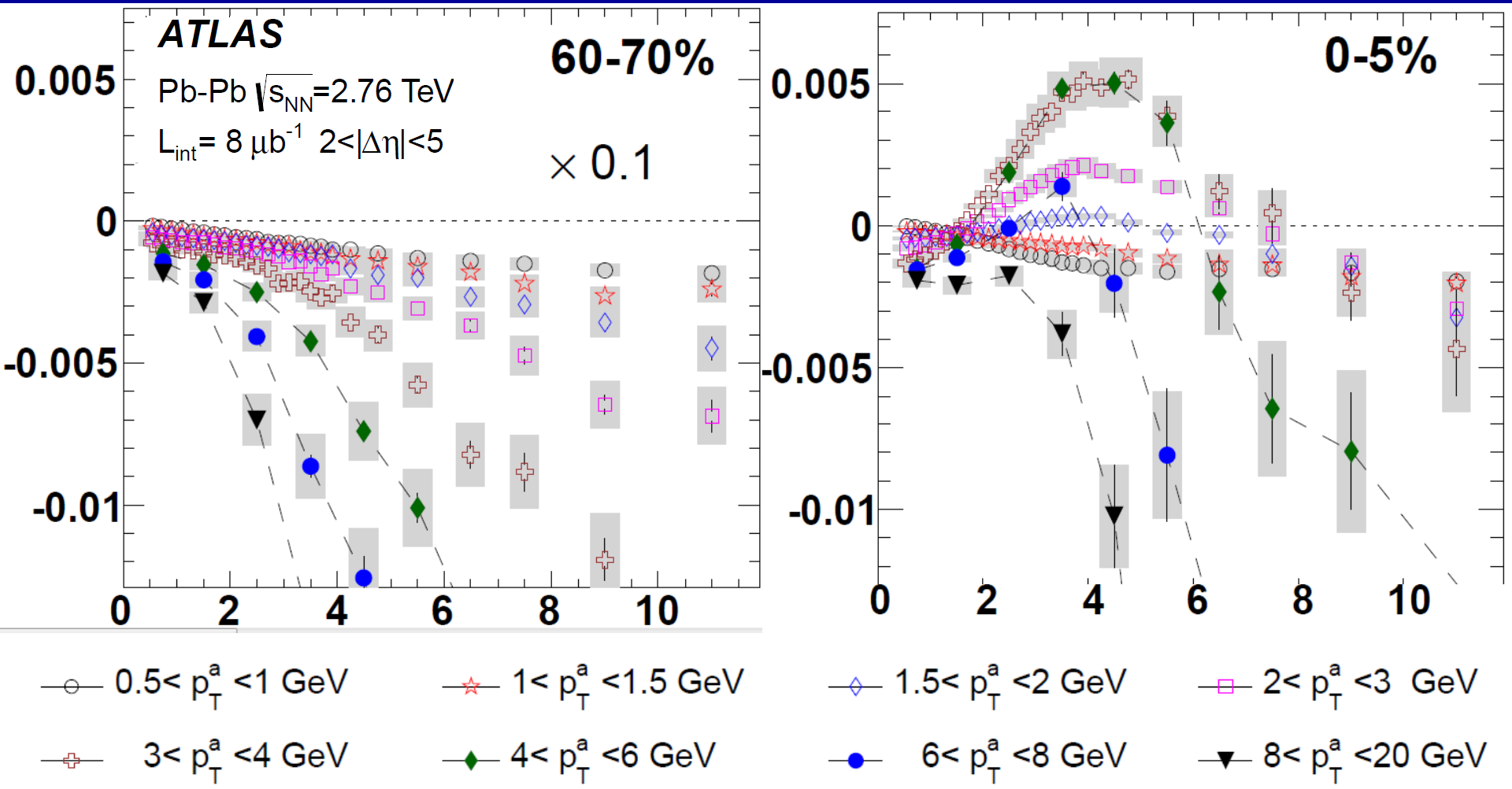


- $v_{1,1}(p_T{}^a, p_T{}^b)$ in peripheral and central event classes from Pb+Pb collisions.
- In central event class the non flow contributions are suppressed.

# Dipolar flow in Pb+Pb (II)

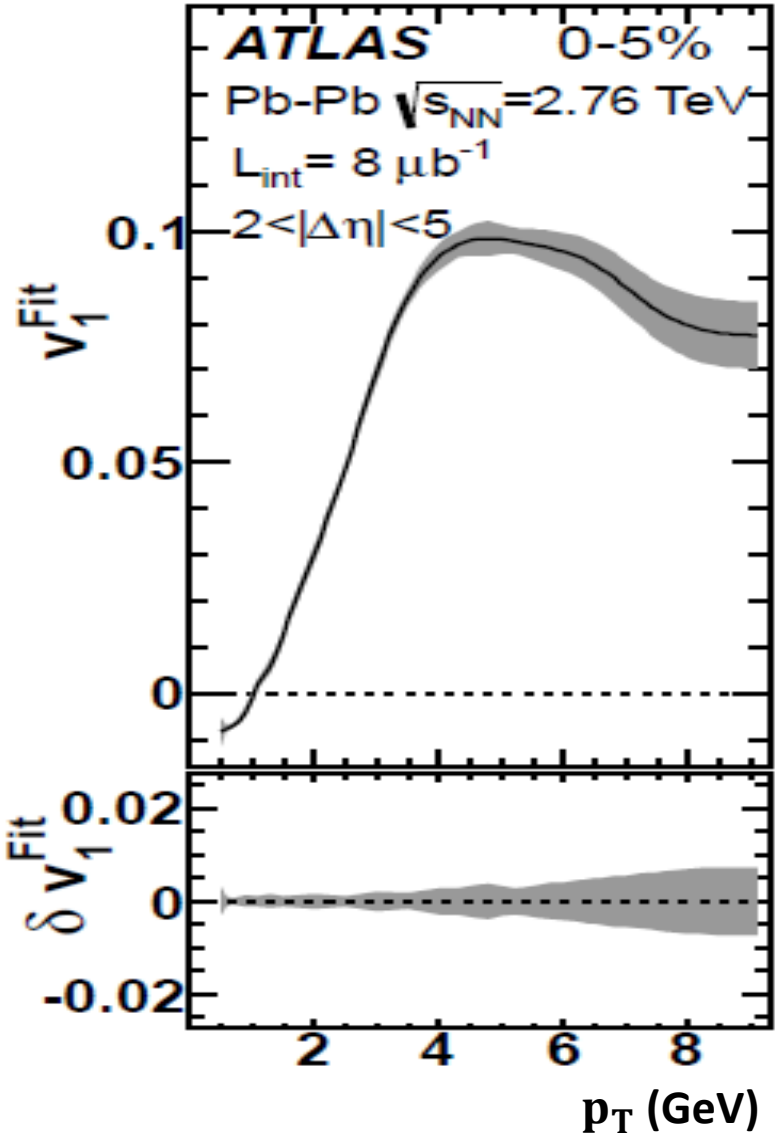


- $v_1(p_T)$ in Pb+Pb obtained from a simultaneous fit to $v_{1,1}(p_T{}^a, p_T{}^b) = v_1(p_T{}^a)v_1(p_T{}^b) - Kp_T{}^a p_T{}^b$
- Negative at low $p_T$ and positive at higher $p_T$
- Changes sign between 1 and 1.5 GeV

# Compare to ridge in peripheral Pb+Pb collisions

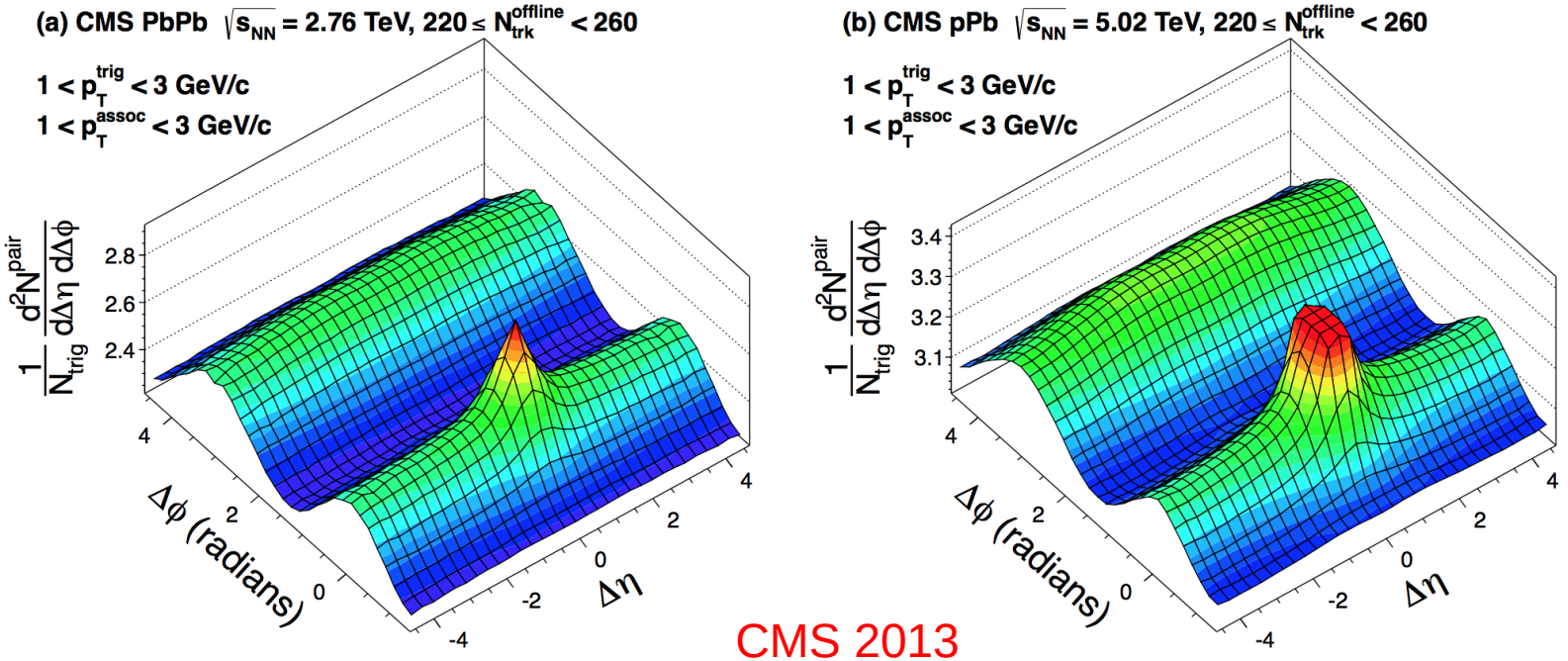


CMS 2013

- Larger jet contribution in similar muliplicity selected p+Pb collisions.

# Away side – Near side (II)

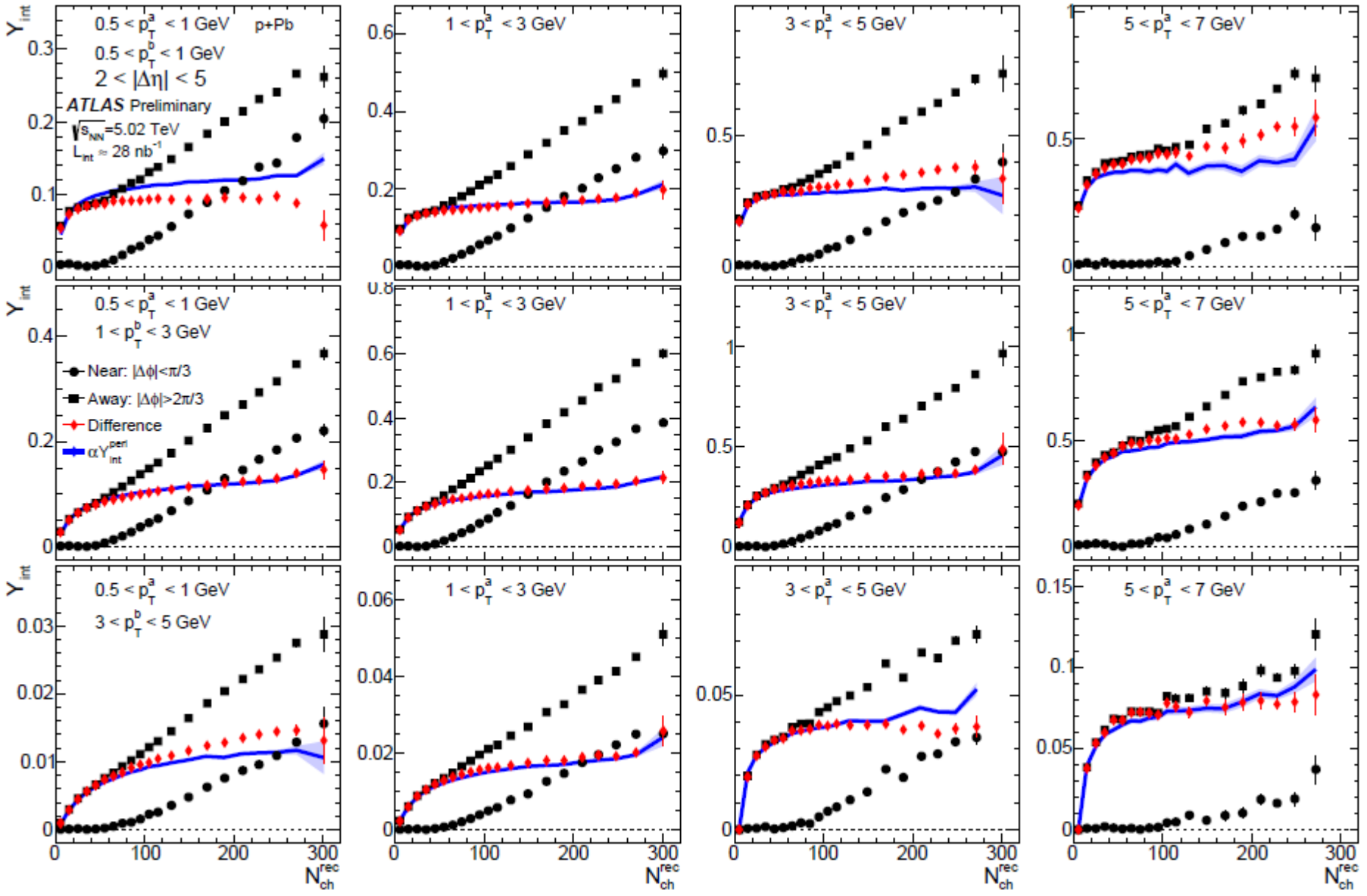

# Ridge at high $p_T$ (II)

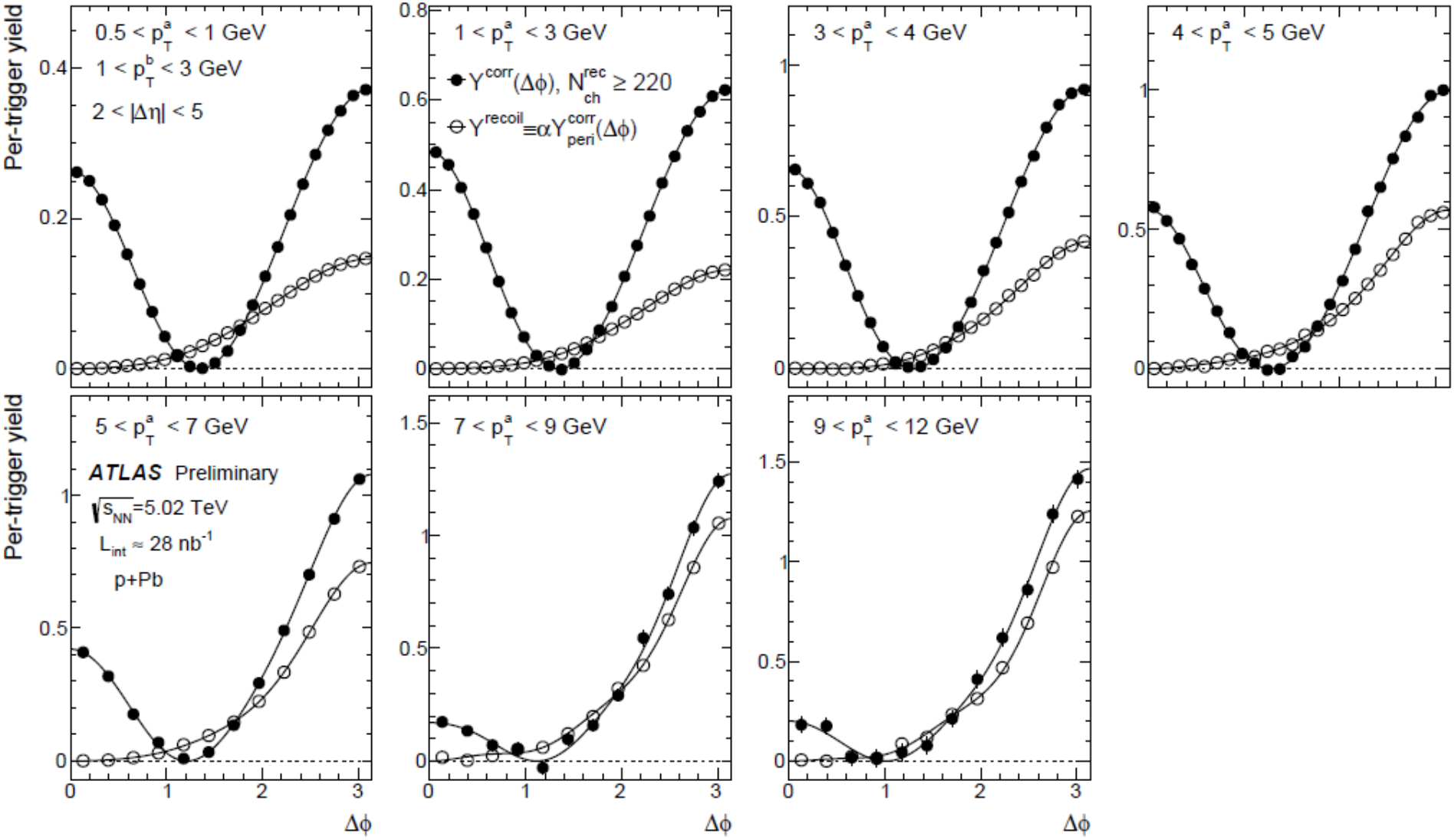


- Near side ridge is visible through the entire $p_T{}^a$ range studied.
- Yield on the away side is also larger than the recoil component.

# Integrated yield vs $p_T$ (II)

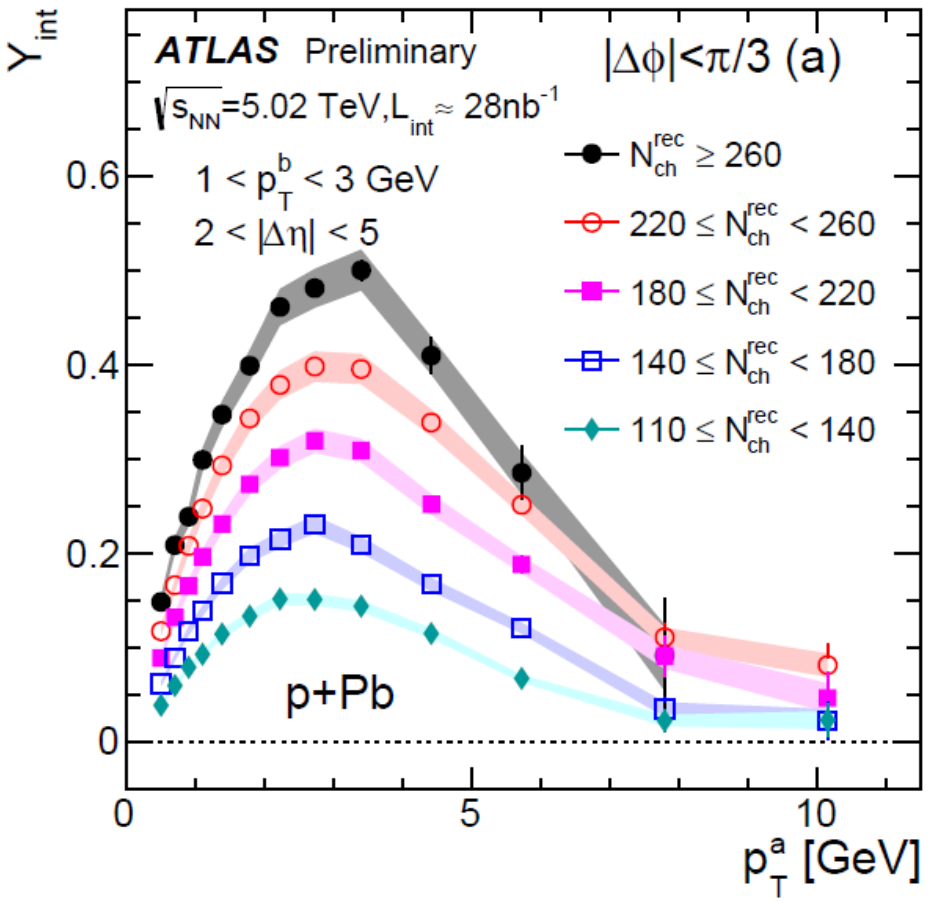


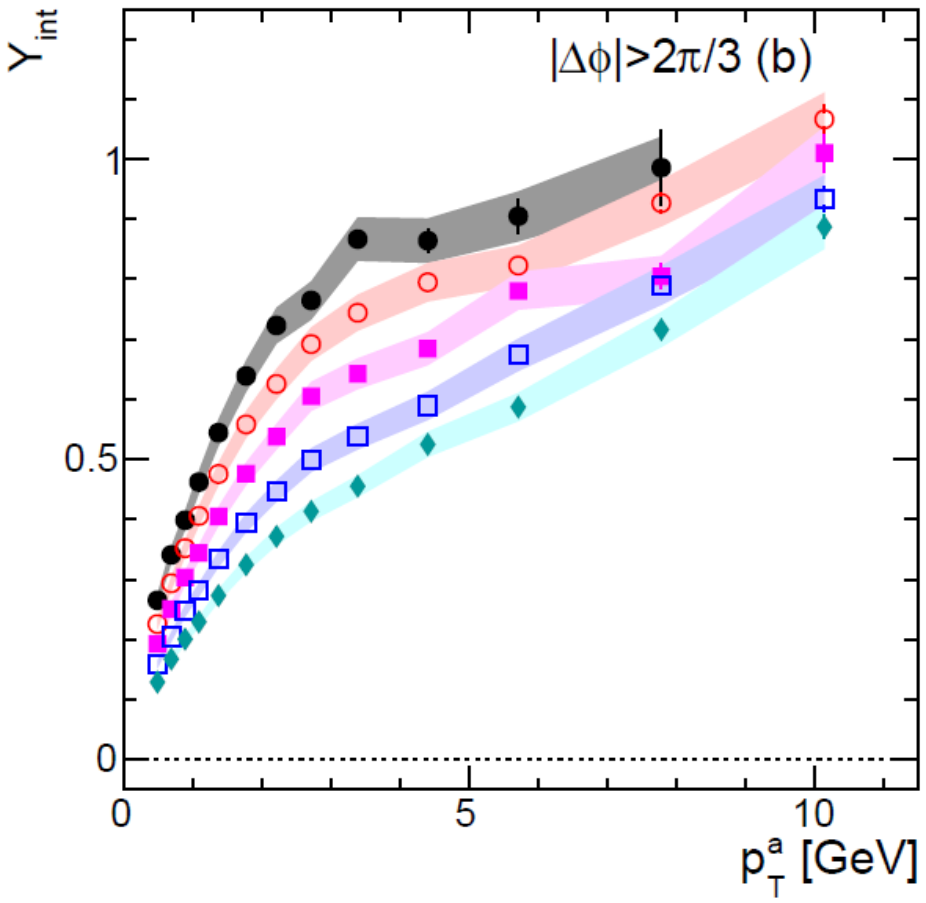


$$Y_{int} = \int_a^b Y^{corr}(\Delta\phi)\, d\Delta\phi$$

- Integrated yields above ZYAM background on the near side and away side.
- Near side yield increases with $p_T$, reaches maximum around 3 - 4 GeV and then decreases.
- Away side yield has large contribution from recoil component.

# Ridge at high $p_T$, $E_T{}^{Pb}$ class

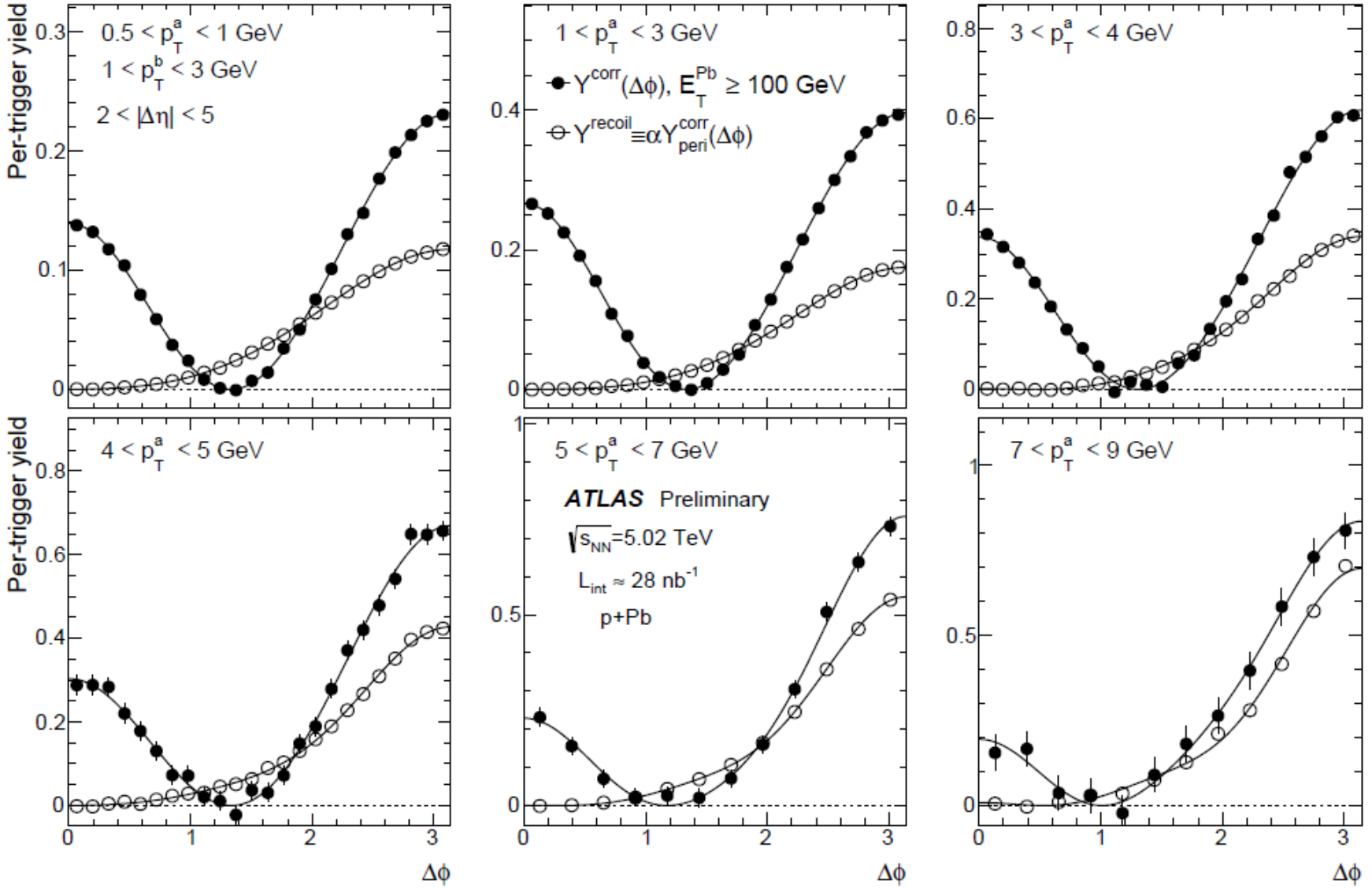

# $v_n$ vs $p_T$, $E_T^{Pb}$ classes